AN EXPERIMENTAL STUDY ON OPTIMIZATION OF Pt-BASED TRIMETALLIC WGS CATALYSTS

by

Bahar Kesim

B.S., Chemical Engineering, Istanbul University, 2014

Submitted to the Institute for Graduate Studies in
Science and Engineering in partial fulfillment of
the requirements for the degree of
Master of Science

Graduate Program in Chemical Engineering

Boğaziçi University

2017

to my family

ACKNOWLEDGEMENTS

First, I would like to express my truthful gratitude to my thesis supervisor Prof. Ahmet Erhan Aksoylu, who guided me throughout my thesis with an immense knowledge and who trusted in me. It was a privilege for me to work with him since he did not hesitate to spend his valuable time and also share his wisdom in catalysis and reaction engineering.

I would like to express my sincere appreciation to Burcu Selen Çağlayan who deserve special thanks for her huge help throughout my work. I also would like to thank her for her expertise and efforts guidance in X-Ray Photoelectron Spectroscopy (XPS) and Raman Spectroscopy analyses.

I would like to express my sincere appreciations for the members of thesis committee Prof. Ramazan Yıldırım and Assoc. Prof. Alper Uzun for accepting to be a member of the examining committee and for kindly revising and commenting on my thesis.

Heartfelt thanks should be addressed to my special friends Özgü Özer for her endless help and everlasting friendship and H. Merve Can for our joyful memories. Deepest thanks to Hakan Şimşek for his encouragement and understanding. He has always been there to support me and cheer me up whenever I was in need. I would like to express my heart-felt gratitude to him.

I also would like to thank Melek Selcen Başar, Merve Eropak, Ali Uzun and Burcu Acar who guided me whenever I needed and also for their friendship. I was very lucky to work with the CATREL team and thus I would like to thank all team members for their support.

I wish to express my thanks to Bilgi Dedeoğlu for his technical assistance and for his help whenever I needed for my reactor system. I also would like to thank Yakup Bal, Melike Gürbüz and Başak Ünen for their friendly and helpful behaviour.

Heartfelt thanks to my dearest family, my mother Serihan Kesim and my sister Yeliz Kesim for their patience, encouragement and continuous support throughout my whole life. Their endless love and trust in me motivated me all the time.

The financial support provided by TÜBİTAK through project 214M170 is greatly acknowledged.

ABSTRACT

AN EXPERIMENTAL STUDY ON OPTIMIZATION OF Pt-BASED TRIMETALLIC WGS CATALYSTS

The overall purpose of this study is to design and develop Pt-based, CeO_2 supported trimetallic Pt-Re-V/CeO_2 catalysts(s) having high WGS activity, selectivity and stability with suppressed methanation under realistic feed *(i.e. feeds simulating typical reformer outlet)* flow in HTS-LTS transition temperature region, allowing the use of a single WGS reactor in fuel processors. In this context trimetallic Pt-Re-V/CeO_2 catalysts prepared by incipient to wetness impregnation were characterized and tested for their WGS reaction performance. In the performance tests, metal loading levels, feed composition and temperature were used as the experimental parameters. Both freshly reduced and spent catalysts were characterized by XPS and Raman spectroscopy analyses. The results revealed that 1Pt-0.5Re-1V/CeO_2 and 1Pt-0.5Re-0.5V/CeO_2 have great potentials to be used in a fuel processor as the WGS catalyst owing to their high activity, stability and selectivity. Another important point is that those catalysts can make the use of a single stage WGS unit in an FP instead of conventional two stage (HTS and LTS) WGS unit. XPS analysis reported Ce^{3+} content is slightly higher in the case of the catalysts with higher WGS activity since Ce^{3+} plays a crucial role in increasing electron transfer ability from support to metallic sites and Ce^{3+} ions are highly active towards reactants due to excess electrons that are left behind when an oxygen atom is removed. Raman spectroscopy results showed no detectable bands for bulk V_2O_5 crystals in any of the samples. This result indicates that vanadium is highly dispersed at the surface without bulk V_2O_5 formation. XPS and Raman spectroscopy results showed the formation of $CeVO_4$ species and VO_2 compound, which has been reported to have promotion effect in the WGS activity, were present on the catalyst. Raman results also revealed the existence of polyvanadate surface species in the catalyst. Moreover, no coke formation was observed on any spent samples.

ÖZET

Pt-BAZLI ÜÇ METALLİ WGS KATALİZÖRLERİNİN OPTİMİZASYONU ÜZERİNE DENEYSEL ÇALIŞMA

Bu çalışmanın amacı yüksek su-buhar geçiş (WGS) aktivite ve kararlılığına sahip, ikincil metanasyon aktivitesini baskılayan, Pt bazlı katalizörler tasarlamak ve geliştirmektir. Bu bağlamda üç metalli Pt-Re-V/CeO_2 katalizörü HTS-LTS sıcaklık geçiş bölgesi için ardışık emdirilme yöntemiyle hazırlanmıştır. İndirgenmiş ve kullanılmış katalizörlerin XPS ve Raman spektroskopisi ile karakterizasyonları yapılmıştır. Performans testlerinde metal yükleme seviyesi, besleme akımı kompozisyonu ve sıcaklık deneysel parametreler olarak kullanılmıştır. Test sonuçları ışığında, yüksek aktivite, seçimlilik ve kararlılık değerlerine bakıldığında, 1Pt-0.5Re-1V/CeO_2 ve 1Pt-0.5Re-0.5V/CeO_2 katalizörlerinin yakıt işlemcisinin WGS katalizörü olarak kullanılma potansiyellerinin olduğu görülmüştür. Diğer önemli nokta ise bu katalizörler olası yakıt işlemcisinde iki aşamalı geleneksel WGS ünitesi yerine tek aşamalı WGS ünitesinde kullanılabilirler. Ce^{3+}, katalizörün destek materyalden metalik kısımlara elektron transfer yeteneğini arttırdığından ve oksijen atomu çıkartıldığında girenler tarafındaki geride kalmış fazla elektronlara göre fazlaca aktif olduğundan, XPS analizi Ce^{3+} miktarının katalizörün WGS aktivitesinin yüksek olduğu durumlarda fazla olduğunu belirtmiştir. Raman spektroskopi sonuçlarında fark edilebilir V_2O_5 kristallerine hiçbir katalizörde rastlanmamıştır. Bu sonuç vanadyumun yüzeyde oldukça iyi dağıldığını göstermektedir. XPS ve Raman spektroskopisi sonuçları beraber incelendiğinde, katalizör üzerinde $CeVO_4$ oluşumları görülmüştür. Raman spektrospi sonuçları katalizör üzerinde polivanadat yüzey oluşumlarının varlığını da belirtmiştir. Ek olarak, kok oluşumu hiçbir kullanılmış katalizör üzerinde görülmemiştir.

TABLE OF CONTENTS

.

LIST OF FIGURES

LIST OF TABLES

LIST OF SYMBOLS

F	Molar flow rate
$F_{i,in}$	Molar flow rate of species i in the feed stream
$F_{i,out}$	Molar flow rate of species i in the product stream
m_{cat}	Catalyst weight
P	Pressure
R	Universal gas constant
T	Temperature
V_{gas}	Volumetric flow rate of the gas
wt	Weight
ΔH°_{298}	Standard enthalpy of reaction

LIST OF ACRONYMS/ABBREVIATIONS

ATR	Autothermal Reforming
DI	Deionized
DSS	Daily Start-Up and Shut-Down
FC	Fuel Cell
FP	Fuel Processor
FTIR	Fourier Transform Infrared Spectroscopy
GC	Gas Chromatograph
GHSV	Gas Hourly Space Velocity
HPLC	High Performance Liquid Chromatography
HTS	High Temperature Shift
LTS	Low Temperature Shift
MFC	Mass Flow Controller
OSC	Oxygen Storage Capacity
PEMFC	Proton Exchange Membrane Fuel Cell
PGM	Platinum Group Metal
POX	Partial Oxidation
PROX	Preferential Oxidation
RF	Real Feed
RWGS	Reverse Water Gas Shift
SR	Steam Reforming
TCD	Thermal Conductivity Detector
TOF	Turn-over Frequency
TOS	Time-on-stream
WGS	Water-Gas Shift
XP	X-Ray Photoelectron
XPS	X-Ray Photoelectron Spectroscopy

1. INTRODUCTION

In a fast changing world, one of the most important issue is satisfying drastically increased energy demand. In course of time, it has become a challenge to fulfill the expanding needs of increasing human population. Electricity has become a major energy form. In order to satisfy the energy demand of the world, approximately 10 terawatt (TW) clean power need to be supplied. Due to the availability and convenient usage of fossil fuels, ~65% global energy is received by oil, natural gas and coal. However, emission and global warming hazards, limited reserves of fossil fuels and increase in the petroleum prices can be listed as side effects (Sharma *et al*., 2015).

Hydrogen is a clean and renewable energy source since it can be used as a solution for clean energy production. High energy carrier feature of hydrogen makes it a tremendous choice for power generation systems. Hydrogen can be generated from renewable technologies such as water splitting or biomass. However, large scale production units of these technologies are hard to implement. Along with the advancement in research, technological development and proliferated use of hydrogen-based energy production ways, including polymer electrolyte membrane fuel cell (PEMFC), the demand for hydrogen is expected to rise drastically. Since fully renewable routes are not yet economically feasible, fuel processors are viable alternative for hydrogen production from hydrocarbons (Sharma *et al*., 2015; LeValley *et al*., 2014).

Fuel cells, which generate electricity from hydrogen considered as one of the most promising way for clean energy production in a foreseeable future. High energy efficiency and low greenhouse gases release feature makes fuel cells to receive extensive attention. On the basis of energy efficiency, PEMFC is believed to be the most convenient fuel cell type for small scale stationary power production since it uses hydrogen and oxygen as the only reactant (Budzianowski *et al.,* 2010; Tanksale *et al*., 2010; Galvita and Sundmacher, 2007).

Catalytic processes used in the production of hydrogen for PEMFC from hydrocarbons have attracted huge attention. However, hydrogen storage and distribution networks still exist as unsolved problems. Hydrogen, as the only fuel of PEMFC, is generally produced by fuel processors (FPs). PEMFC anode catalyst is poisoned in CO rich medium however fuel processors have the advantage of producing H_2 rich feed with less than 40 ppm CO. Fuel processors include three serial catalytic units, reforming, water gas shift (WGS) and preferential oxidation (PROX). As the first catalytic unit of fuel processors, reformer converts hydrocarbons to CO, H_2, H_2O and CO_2. The reformer product mixture, which generally contains 10% CO, is fed to WGS unit. WGS reaction is employed to decrease CO level while increasing H_2 concentration simultaneously. In the following PROX unit, quantity of CO is lowered further to required ppm levels. At the exit of FP, carbon monoxide level should not be over 40 ppm (Galvita and Sundmacher 2007; El-Moemen *et al*., 2010).

WGS reaction has been used in industrial processes over 40 years. It has become to play more crucial role since it was reported as a source of hydrogen for Haber process. WGS is a reversible and exothermic reaction which converts CO and H_2O into CO_2 and H_2. In other words, it produces additional H_2 at the end of the reaction of steam with CO (Ratnasamy and Wagner, 2009).

WGS reaction is moderately exothermic; with decrease in temperature equilibrium conversion and H_2 production increases. However, reaction is getting faster at high reaction temperatures. To overcome these thermodynamic and kinetic limitations, industrial WGS units have two serial adiabatic WGS reactors which are operating at different temperatures in fuel processors. High temperature shift (HTS) reactor operates over 300 °C and uses iron/chromium based catalysts whereas low temperature shift (LTS) reactor operates below 250 °C and uses copper/zinc based catalysts. In general, HTS reactor decreases CO level from ca. 15% down to ca. 3% and LTS reactor reduces CO level to nearly to 0.4% (Chen *et al*., 2010).

Both HTS and LTS catalysts require complex reduction procedures for their activation. The Fe_2O_3/Cr_2O_3 catalyst, which operates at high temperatures, suffers from

rapid deactivation at the initial steps of the reaction mechanism. $Cu/ZnO/Al_2O_3$ can also be deactivated at low temperatures by sulphur containing species when a sulfur containing raw material is used as feed stream for reformers. In addition, they do not have enough mechanical stability during daily start-up/shut-down (DSS) operations, and also they deactivate on exposure to air or water. Additionally, occurrence of deactivation due to poisoning is another problem. As a result, as it is seen, conventional industrial WGS catalysts are not suitable for FP-PEMFC operations (Kugai *et al*. 2011; Yu *et al*., 2006).

In many studies, platinum-group metal (PGM) based and reducible oxide supported catalysts provide promising results for WGS reaction. Pt and Au based WGS catalysts are effective for being non-pyrophoric and poison resistant metals. Low methanation activity, high hydrogen selectivity and thermal stability are other criterions for efficient WGS fuel processor catalysts. Additionally, instead of two stage WGS reactors in conventional systems, it is beneficial to use a single stage WGS reactor for FP-PEMFC applications operating in medium temperatures as 250 and 300 °C (Zhu *et al*., 2011; Xu *et al*., 2012; LeValley *et al.,* 2014; Çağlayan and Aksoylu 2011).

The aim of the current work is to design and develop Pt-based, CeO_2 supported trimetallic $Pt\text{-}Re\text{-}V/CeO_2$ catalysts(s) having high WGS activity, selectivity and stability with suppressed methanation under realistic feed *(i.e. feeds simulating typical reformer outlet)* flow in HTS-LTS transition temperature region, allowing the use of a single WGS reactor in fuel processors. In this context, several $Pt\text{-}Re\text{-}V/CeO_2$ catalysts with different Pt, Re and V loadings were developed, characterized and tested for their performances in WGS reaction. There, Re was used to modify the electronic structure of Pt, while V was added as a third metal/promoter aiming to benefit from the involvement of oxygen bridge formations, V-O-Ce and V-O-V, in WGS surface reaction. In the studies, catalyst composition (i.e. Pt:Re:V loading ratios), temperature (300, 350 and 400 °C) and H_2O/CO feed ratio in possible realistic feeds were used as the experimental parameters. Activity, selectivity, and stability of the catalyst samples were considered as the performance criteria. X-ray photoelectron spectroscopy (XPS) was used to analyze the

oxidation states of the metals and support, and Raman spectroscopy was used in order to examine the possible V-O-V and V-O-Ce bonds.

Section 2 of this work involves detailed information about fuel processors and WGS catalysts. The experimental system carried out is presented in detail in Section 3. The characterization tests and obtained results are showed and discussed in Section 4. Finally, Section 5 includes the conclusions from the present study and recommendations for the future work.

2. LITERATURE SURVEY

2.1. Hydrogen and Fuel Processors

Hydrogen is one of the most common elements in Earth's crust and it is the simplest element of periodic table. It is considered as a cost-attractive energy carrier with its nonpolluting and inexhaustible feature. Hydrogen as a clean energy, burns with oxygen cleanly, producing water (vapor) as the only product. As burning hydrogen is an environmental friendly and clean energy production route, it is widely accepted as a potential ideal energy carrier for sustainable fuel cells and decentralized energy production systems (Navarro *et al*., 2007).

Electricity, one of the most required energy types, can be produced by fuel cell technology. The proton exchange membrane fuel cells (PEMFCs) are the most promising alternatives for small scale applications with their high power density, fast response and modularity characteristic. PEMFC technology is using hydrogen for the production of electricity without any harmful gas emissions because of its high reactivity at the anode side of fuel cells. Along with the storage difficulties; production and distribution drawbacks lead to look for an efficient and compact device for the production of hydrogen from resources which are both fossil and non-fossil (Avci *et al*., 2001; Çağlayan *et al.*, 2005).

Fuel processor (FP) PEMFC systems which are capable of producing H_2 from hydrocarbons with wide distribution networks onsite, are the most ideal option for small scale stationary PEMFC applications. Fuel processor is a CO free hydrogen production system which has three main catalytic processing series; reforming, water-gas shift (WGS) and preferential CO oxidation (PROX) (Gökaliler *et al*., 2008).

As the first catalytic unit of fuel processors, reformer converts hydrocarbons to CO, H_2, H_2O and CO_2 (Galvita *et al*., 2007). A wide range of feed stocks (methane, ethane, higher hydrocarbons, etc.) can be utilized in the reformer. Besides these vast alternatives,

gaseous fuel reforming is the current leading source for the hydrogen production. Reforming can take place in three different production routes, steam reforming, partial oxidation (POX) and oxidative steam reforming:

$$CH_4 + H_2O \leftrightarrow CO + 3H_2 \qquad \Delta H^{\circ}_{298} = 206.2\ \text{kJ/mol} \qquad (2.1)$$

Steam reforming (SR) (Equation 2.1) is an extremely endothermic reaction that operates poorly at low temperatures since the reaction requires high energy input and high temperatures in the range of 700-1000 °C. Besides their prone feature to sulfur poisoning, carbon formation and sintering during operations; their low price and high activity make Ni based catalysts the widely used and studied catalysts for SR reaction (LeValley *et al.*, 2014; Shekhawat *et al.*, 2011).

Combining Partial Oxidation (POX) with SR which is called oxidative steam reforming is a well-preferred alternative for ensuring high energy demand of SR. Pt-based catalysts are the most commonly used and active catalysts for POX. POX uses oxygen for converting alkanes into hydrogen and carbon monoxide (Equation 2.2) (Shekhawat *et al.*, 2011):

$$CH_4 + 0.5\ O_2 \leftrightarrow CO + 2H_2 \qquad \Delta H^{\circ}_{298} = -35.6\ \text{kJ/mol} \qquad (2.2)$$

Water Gas-Shift reaction (Equation 2.3) is a key step in fuel processors. It is a well-known process to increase hydrogen yield from reformer while reducing CO content in the effluent stream (Aranifard, 2013):

$$CO + H_2O \leftrightarrow CO_2 + H_2 \qquad \Delta H^{\circ}_{298} = -41.2\ \text{kJ/mol} \qquad (2.3)$$

In fuel processors by the help of WGS unit CO concentration decreases from 5-10% to less than 1% (Natesakhawat *et al*., 2006). Water gas-shift is thermodynamically favored at low temperatures and a pressure independent reaction. The common practice for the WGS reaction is a two-stage shift reactor. While high temperature shift step which operates at 350-500 °C decreases CO level to 2-3% when gas steam is cooled to

ca. 200 °C, low temperature shift reaction reduces CO concentration to 1%. In industrial applications Fe-Cr oxide and $Cu/ZnO/Al_2O_3$ catalysts are used for high temperature and low temperature shift reactions, respectively (Lee and Chu, 2003).

After WGS unit of the fuel processor, the effluent steam still contains about 1% CO which is too high for the operation of PEM fuel cell. It is essential to reduce CO levels to less than 10 ppm (Gökaliler *et al.*, 2008) since the Pt-based electro catalyst of the PEMFC anode is poisoned by CO. Preferential oxidation is performed to reduce CO level about 10 ppm before H_2-rich product reaches to fuel cell. Proper heat displacement is playing a crucial role in PROX reactions (Equation 2.4) due to its highly exothermic feature. (Lee and Chu, 2003):

$$CO + 0.5\ O_2 \rightarrow CO_2 \qquad \Delta H^{\circ}_{298} = -283.6\ \mathrm{kJ/mol} \qquad (2.4)$$

In order to reduce the CO concentration and minimize the undesirable hydrogen oxidation (Equation 2.5), PROX catalyst should be highly selective and should operate at ca. 130 °C (Dudfield *et al*., 2001). Low Pt containing γ-alumina supported catalysts are commonly used for PROX reactions due to Platinum's ability to adsorb CO (Lee and Chu, 2003):

$$H_2 + 0.5\ O_2 \rightarrow H_2O \qquad \Delta H^{\circ}_{298} = -243.5\ \mathrm{kJ/mol} \qquad (2.5)$$

The commercial catalysts of the mentioned reactions above are not suitable for small scale mobile/immobile fuel processing devices since they require special activation procedures and there is a technical complexity about to startup–shutdown cycles. Taking into account the desired low CO levels for the optimum operation conditions of PEMFC; there is still a vast research and development area in fuel processor operations (LeValley *et. al*., 2014).

2.2. Water Gas Shift (WGS) Reaction

2.2.1. General Information about WGS Reaction

Water Gas Shift (WGS) (Equation 2.6) is an exothermic and equilibrium limited reaction which converts carbon monoxide and steam to hydrogen and carbon dioxide:

$$CO + H_2O \leftrightarrow CO_2 + H_2 \qquad \Delta H^{\circ}_{298} = -41.2\ \text{kJ/mol} \qquad (2.6)$$

As it is first reported in 1888, WGS is a critical hydrogen generation reaction. It is reversible and mildly exothermic. Equilibrium constant of WGS is higher at low temperatures, however high temperatures lead to fast kinetics and enhanced reaction rates. (Kugai *et al*., 2011a).

WGS reaction is extensively used in the industry for the manufacture of ammonia, methanol and hydrogen (hydrotreating, hydrocracking of petroleum fractions and other hydrogenations in the petroleum refining and petrochemical industry). It also has a wide area of usage at hydrocarbons (by the Fischer-Tropsch process) and metals (by the reduction of the oxide ore) (Ratnasamy and Wagner, 2009).

WGS decreases CO level of the reformer outlet while increasing H_2 concentration to the desired levels. CO conversion is strongly limited by kinetics at low temperatures and by thermodynamics at high temperatures due to mildly exothermic feature of WGS reaction. To handle these limitations in industrial operations, WGS takes place in two reactors in series: High temperature shift (HTS) and low temperature shift (LTS) reactors (Zhu *et al*., 2011). Conventional high temperature shift reaction catalyst is Fe_3O_4/Cr_2O_3, which provides fast reaction kinetics and operates between 350-500 °C to convert CO up to 15%. These catalysts are best known for their economical price, sulphur resistant feature and long life ability. On the other hand they are not active enough below 350 °C. In the second stage of industrial operations, low temperature shift catalyst $Cu/ZnO/Al_2O_3$, operates at 180-240 °C range and reduces CO level down to nearly 0.4%. As Cu-Zn based catalyst shows good activity only at low temperatures, these commercial

catalysts are not suitable for the application at conditions above 300 °C. Besides, they are pyrophoric, sensitive to startup–shutdown cycles, intolerant to poisons and oxidation and they require special activation procedures. To sum up, researchers are trying to find new catalyst formulation to overcome the above mentioned problems to provide stable operation at PEMFC-FP systems (LeValley *et. al*., 2014; Trimm, 2005). The catalysts should not yield to methanation reaction (Equation 2.7), which consumes valuable hydrogen additionally (Park *et al*., 2008):

$$CO + 3H_2 \leftrightarrow CH_4 + H_2O \qquad \Delta H^{\circ}_{298} = -205.81\ \text{kJ/mol} \qquad (2.7)$$

The 50% of the entire volume of fuel processors are occupied by the shift reactor; thus using a single reactor operating at mid-temperatures instead of two shift stages is also another innovation field to be developed (Lee and Chu, 2003).

2.2.2. Conventional Fe- and Cu-based Catalysts of WGS Reaction

There are many studies and reports in literature concerning of explaining the operation conditions and the working principles of HTS Fe-based and LTS Cu-based catalysts (Lee *et al*., 2013; Maraño *et al.,* 2009; Ruettinger *et al*., 2006; Gawade *et al*., 2010).

HTS reactor, which is the first step of a WGS unit, involves iron oxide and stabilized by chromium oxide as commercial catalyst. Fe_3O_4/Cr_2O_3 was patented by Bosch and Wild in 1914 and has a wide range of use in industrial operations in the temperature range of 350-500 °C (Ruettinger *et al*., 2006). The studies examined below mainly focuses on the preparation procedures and the effects of Cr on HTS catalysts.

Investigation about the behavior of Cr-free Fe-based catalyst prepared through propylene oxide-assisted sol-gel technique was studied in the literature (Gawade *et al*., 2010). The study revealed that using propylene oxide technique was more eco-friendly than habitual sol-gel preparation method. The optimum Fe/Cu ratio was obtained as 5 and excess copper amount caused significant decrease in WGS selectivity. They also

reported that increase in the water amount in the feed stream resulted CO conversion enhancement.

The effect of different preparation methods for Fe-Cr based WGS catalysts was investigated (Maroño *et al*., 2009). Oxidation-precipitation and co-precipitation methods were used as preparation procedures. Results showed oxidation-precipitation method provides highly active Fe-Cr based catalyst.

Based on the study of Natesakhawat *et al*. activity improvement of Fe-Al catalysts in WGS reaction was succeed by addition of small amount of cobalt or copper. The study showed that Al and Cr prevents catalyst from sintering and promotes the catalytic activity. The promotion feature of Cu decreased when the temperature increased. Their results also pointed out the importance of the catalyst preparation method and how it plays a crucial role for the promotion effect of Cu (Natesakhawat *et al*., 2006).

Experimental investigation of the effect of alumina has been studied by Popa *et al*. In that study Fe-Al-Cr-Cu and O containing catalysts were synthesized by the co-precipitation method for observing the enhancement effect of alumina. According to the obtained results, 15 wt.% addition of alumina positively affected both the conversion rates of CO and thermal stability. CO conversion rates of CO were 73.8% larger than the reference catalyst with no alumina. However, their results also showed that alumina by only itself could not effectively stabilize Fe_3O_4 (Popa *et al*., 2010).

Copper-based catalysts have been used in LTS reaction since the 1960s. $Cu/ZnO/Al_2O_3$ operates at 180-240 °C and reduces to CO content of reformate to < 0.5% (Ruettinger *et al*., 2006). There are many studies in literature that investigate the effects of Cu loading, preparation method and support on the LTS activity of the $Cu/ZnO/Al_2O_3$ catalyst (Kam *et al.*, 2010; Guo *et al.*, 2009a).

Nishimura *et al*. carried out a study about the effects of preparation methods and calcination temperature for catalysts' activity and stability during Daily Start-Up and Shut-Down (DSS) operations. The Cu/Al_2O_3 which was prepared by co-precipitation

technique among homogenous precipitation, sol-gel and impregnation methods and calcined at 823 K showed the highest sustainability and activity even after 50 cycles. (Nishimura *et al*., 2010).

Guo *et al.* (2009a) conducted a study on the deactivation of LTS catalyst $Cu/ZnO/Al_2O_3$. During start-up/shut-down operation for mobile systems they pointed out that the formation of $Zn_6Al_2(OH)_{16}CO_3 \cdot 4H_2O$ was the real reason for the blockage of the active sites and caused degeneration under cyclic operations. They also mentioned the most convenient calcination temperature and preparation method for the best activity and stability was 450 °C and co-precipitation, respectively.

Requirement for specific reduction procedures, safety cautions on pyrophoricty are the drawbacks for commercial WGS catalysts. Even though they are suitable and well-controlled for industrial hydrogen production systems they cannot satisfy the requirements of the PEMFC systems. The main focus of this work is to answer the purpose of finding a non-pyrophoric catalyst which is sufficient to daily start-up/shut-down cycles and being able to work in a significant reactor size. According to literature (Castaño *et al*.) platinum-group metal (PGM) based catalysts supported on reducible oxides are suitable catalyst systems which can satisfy these needs (Castaño *et al*., 2014).

2.2.3. Platinum-Group Metal (PGM) Catalysts of WGS Reaction

Catalytic researches are carried out and experiments have been done to find suitable bimetallic/multi metallic catalysts for WGS reaction. Recent works known from the studies of LeValley *et al*. (2014) focused on Rh, Ru, Ir, Au, and Pd which play critical roles as active metals in fuel cell applications. According to Fu *et al*. (2001), platinum group metals supported with ceria were found as leading candidates for catalytic converters and they attracted huge attention of automobile industry.

The catalytic activities of noble metal activated catalysts were investigated for water gas shift reaction in the studies of Panagiotopoulou *et al*. (2006). The reactions were taking place in the temperature range of 150-550 °C. The precious metals among all

metal support combinations displayed higher activity when supported with “reducibles” (TiO_2, CeO_2, La_2O_3, and YSZ) than “irreducible” oxides (Al_2O_3, MgO and SiO_2). Among the studied metallic phases (Rh, Ru, and Pd); also from the research of Radhakrishnan *et al*. (2006a) among Ru, Rh, Ir, and Au active metals; Pt were found as the most active and the most promising precious metal for WGS reaction.

Some studies (Lenite *et al.*, 2011) were also available on the catalytic activity of Au using (α-γ)-Al_2O_3 and CeO_2 support. The catalysts were synthesized by deposition-precipitation method and experiments were performed by both realistic and ideal reformate feed compositions. In the study, CO conversions were obtained below 30% with gold-alumina catalyst. The accumulation of gold on the support surface was observed as the reason. Lower CO conversion levels were obtained at the realistic reformer outlet when pH values decreased from 10 to 7. However, catalytic activity due to the CO conversion showed satisfactory results with active metal-ceria combination where Au ratio was kept at 3%.

Boaro *et al.* (2009) investigated the effect of ZrO_2 and ceria-zirconia on gold and platinum based catalysts. The feed conditions were same with the autothermal reformer outlet and temperature range was kept between 150-240 °C. According to the article, platinum-based catalysts showed poor activity at low temperatures. Thus, they found that zirconia supported catalyst revealed higher activity in the mentioned temperature range when gold was used as an active metal.

The effect of gold loading on WGS activity studied by Andreeva *et al*. (2002). The deposition-precipitation preparation method was used in the experiment as a preparation procedure. Reactions were taking place in the temperature range of 140-350 °C. The highest activity and stability was achieved with 3%Au/CeO_2 catalyst. Article indicated that both activity and stability of catalyst depends on metal-support interactions. Due to the temperature programed reduction (TPR) results optimal ratio between active metal and support is the reason for oxygen production surfaces which is effecting CO conversion levels positively.

In another study carried out by Çağlayan *et al*. (2011), effect of Re addition on Au/ceria was examined. The reaction temperature was in a wide range of 200-450 °C. Gold addition on impregnated Re/ceria by deposition precipitation technique led high CO conversion levels even at higher H_2O/CO ratios. However, Re impregnation over Au/ceria surface showed poorer water gas shift activity due to the active side blockage of the catalyst. According to the paper, strong Au-Re interactions and high Re dispersions are the reasons for the increment of WGS activity.

Paper of Castaño *et al.* (2014) represented a successful study about the activity of Pt and Au based, CeO_2 and CeFe oxide supported catalyst. A comparative analysis between Au and Pt showed platinum-based catalysts represent higher activity at the temperature above 200 °C when gold-based is successful at lower temperatures around 180 °C. Gold-based catalysts got affected more than platinum-based catalysts from the electronic properties of support material. Besides, platinum showed better tolerance at the changes on feed stream while having high reaction rates. In conclusion, from the experiments, CeO_2 or CeFe oxide supports were found suitable for both gold and platinum systems for high WGS activity.

2.3. Platinum-based PGM Catalysts in WGS Reaction

In many academic works, alternative Pt-based, oxide and mixed oxide supported catalysts have been studied and found as the most promising for WGS reaction. Pt/ZnO (Kam *et al*., 2010), Pt/TiO_2 (Azzam *et al.*, 2007b; Zhu *et al*., 2011), Pt/ZrO_2 (Azzam *et al.*, 2007b), Pt-Ni/Al_2O_3 (Çağlayan *et al*., 2009), Pt/CeO_2-Al_2O_3 (Germani *et al*., 2005), Pt/CeO_2 (Panagiotopoulou *et. al*., 2007; Liu *et al*., 2005) are some studied examples. The detailed results of researches will be specified below.

2.3.1. Applications of Mono and Multi Metallic Platinum-based Catalysts

The comparative study about pyrophoricity and stability of Cu- and Pt-based catalysts studied by Kam *et al*. (2010). Cu/ZnO-based catalyst showed pyrophoricity with a significant temperature increase (up to 350 °C) while no pyrophoric evidence was

found for Pt-based catalysts. During DSS operations Cu/ZnO displayed significant activity lost. Even though Pt/TiO_2 and Pt/ZrO_2 catalysts suffered from serious sintering during steady-state operations, they have been found as the most active catalyst combinations. As the use of reducible oxide support is crucial for Pt activated WGS catalysts, according to the experiments, the support combination for WGS activity of Pt-based catalysts were found as: TiO_2>CeO_2>ZrO_2. Pt activity with the mentioned support combinations (TiO_2, CeO_2, ZrO_2) was also investigated by Azzam *et al.* (2007b). The best activity was achieved with Pt/TiO_2 because the formation of stable carbonate species on CeO_2 caused Pt/CeO_2 deactivation. Re addition prevented Pt sintering where sintering might cause the deactivation of Pt/TiO_2. The studies about the promotion effect of Re are more precisely overviewed in the section 2.4.3.

Pt/ceria/alumina catalyst investigated by Germani *et al*. (2005) to see the catalytic activation of non-pyrophoric catalysts. Reactions were taken place in realistic feed compositions with the temperature range of 300-400 °C. They revealed, change in the amount of ceria effects the behavior of binder during the catalyst preparation. Due to better platinum utilization for the best activity, the pellet forms of catalysts were preferred ones when compared to powder forms of the catalyst samples.

Panagiotopoulou *et. al*. (2007) investigated the effects of doped various cations (Ca, La, Mg, Zn, Zr, Yb, Y, Gd) on Pt/ceria catalysts which were prepared by urea-nitrate combustion method. According to the results, the reducibility and oxygen ion mobility of CeO_2 were affected by promoters which directly affects the WGS activity.

The effect of Na addition to Pt/TiO_2 studied by Zhu *et al*. (2011). Co-impregnation method was used to prepare 1-10 wt.% Na promoted 1 wt.% Pt/TiO_2. It was observed that Na loading significantly affected the 1% Pt/TiO_2 activity. According to the experiments, remarkably high activity values were observed with 3-4 wt.% Na loaded 1% Pt/TiO_2. In addition to provided active sites for WGS reaction, it was stated that the strong metal-promoter interaction also prevented Pt sintering.

Liu *et al*. (2005) focused on the reason behind the deactivation of Pt/CeO_2 catalyst during shutdown/startup cycles. Formation of carbonates on the surface of CeO_2 was found as the main reason. Pt metal surfaces were blocked and electronic properties were limited due to carbonate formation. However, sintering of Pt did not contribute to deactivation under shutdown conditions.

Activity of bimetallic $Pt\text{-}Ni/Al_2O_3$ investigated by Çağlayan *et al*. (2009). Idealized feed compositions were conducted in the temperature range of 200-450 °C. Effect of the promoter of Ni were examined and the increment of Ni content and H_2O/CO ratio were found as the main reasons for shifted carbon monoxide-temperature curve toward lower reaction temperatures. According to results, no methanation formation was detected and $Pt\text{-}Ni/Al_2O_3$ catalysts are highly active and selective for water-gas shift reaction.

2.3.2. Ceria Supported Pt-based WGS Catalysts

Cerium oxide has been playing crucial role in exhaust gases system since the introduction of three way catalysts (TWC) in automobile industry at 1980s (Shelef *et al*., 2002). It has also been used as an emission control component for converters and solid oxide fuel cells. Ability of high oxygen storage capacity (OSC) of ceria comes from the relevant surface defects. That causes enhancement of the reactivity of catalytic reactions. Ceria oxides have been introduced as promoter and promising metal oxide support for noble metal based catalysts in WGS reaction. Mining the literature one can easily be seen, for higher activities, support material should be a reducible oxide to have high redox properties and to have a role as a source of oxygen. (Andreeva *et al*., 2002; Radhakrishnan *et al*., 2006a; Esch *et al.*, 2005; Farias *et al.*, 2008).

The driving force behind the high OSC of ceria is believed the Ce^{4+}/Ce^{3+} redox reaction. The oxygen produced redox process as shown in the Equation 2.8 can be utilized under reduction conditions. Furthermore, contribution of improved dispersion of active metal and the effect of promoter are the other factors for capacity of oxygen storage (Andreeva *et al*., 2002). Both key roles are controlled by the surface defects of oxygen vacancies such as type, size and distribution. On metal oxide surfaces, the

oxygen vacancies are known as the most reactive sites. The surface lattice oxygen atom is usually act as an oxidant when an adsorbate is oxidized and surface oxygen vacancy is generated. The excess electrons of ceria that are left from the removal of neutral oxygen, localize on empty f states. In ceria this situation is resulted as the reduction of Ce^{4+} to Ce^{3+} ions which efficiently enhance the reactivity of the CeO_2 substrates (Esch *et al.*, 2005; Campbell and Peden, 2005). According to Boaro *et al.*, (2009), even though redox properties of support are important; nature of metal-support interface is playing more curial role in the catalyst activity:

$$2CeO_2 \leftrightarrow Ce_2O_3 + {}^1/_2\, O_2 \tag{2.8}$$

It should be mentioned that metal-modified cerium oxides possess higher reducibility and oxygen storage capacity than pure ceria. Another issue must be mentioned is the particle size of ceria. Based on the same study, ceria particle with diameter less than 10 nm have greatly higher conductivity than medium particle ceria size. The addition of La_2O_3 to CeO_2 helped to stabilize ceria particles against sintering and to create oxygen vacancies (Fu *et al*., 2001).

Catalyst combination of Pt-based CeO_2, TiO_2 and mixed CeO_2-TiO_2 in the temperature range of 200-300 °C have been investigated where H_2O/CO is 7. The results showed, catalyst composition depends on the reaction temperature and the feature of support-oxide. From the experiments, primary contribution to turn over frequency (TOF) comes from the particle size of Pt which changed between 1.3 and 8 nm. Moreover, increase in the particle size of platinum and increase in the loading of it led favorable changes on TOF (s^{-1}) and specific reaction rate of WGS reaction (Kalamaras and Gonzalez *et al.*, 2011; Kalamaras *et al.*, 2011).

There are four different reaction pathways for WGS reaction. Among redox route, associative formate route with redox regeneration of oxide support and carbonate route; associative formate route is the prevalent reaction pathway for Pt/CeO_2. Under medium temperature reaction conditions (300 °C) with Pt loading 0.1 to 5 wt.%; activation of

water on support is achieved by the surface hydroxyl group formations on oxides and/or reduced support (Azzam *et al*., 2007a).

2.3.3. Rhenium Promoted Pt-based WGS Catalysts

In the late 1960s Pt-Re/Al_2O_3 has been used as a successful naphtha reforming catalyst with an improved stability. The parameters such as the metal precursor employment, the catalyst preparation procedure, conditions of pretreatment, ratio of Pt and Re and lastly the feature of oxide support have been investigated in order to explain the positive interaction between Pt and Re. (Sato *et al*., 2005; Sato *et al*., 2006; Azzam *et al*., 2007; Iida and Igarashi, 2006; Choung *et al*., 2004; Azzam *et al*., 2013; Azzam *et al*., 2008).

Sato *et al*., (2005) reported a study to understand the effect of Re content on Pt-Re/TiO_2 and Pd-Re/TiO_2. Results showed, Re affected the activity of Pt-Re/TiO_2 more than Pd-Re/TiO_2 whereas the activity of Pt based catalysts mostly depended on temperature. Furthermore, Re addition increased the particle sizes of active metal Pt where the particle size affects the activity positively. Both the stabilization of format species and acceleration of hydrogen formation were announced as the other roles of Re. Another key thing to remember is that the stability of prepared catalysts got improved where sintering is limited by Re (Sato *et al*., 2006; Azzam *et al*., 2007).

Iida *et al.* (2006) performed a research in order to examine the role of Re on Pt/TiO_2 and Pt/ZrO_2 as low temperature WGS catalysts. Due to the TEM micrograph results, dispersion of Pt increased on TiO_2 by the addition of Re. Electronic interaction between Pt and Re played different roles on both catalysts. The interaction between Pt and Re was stronger at TiO_2 supported catalyst than ZrO_2. Re acted as an anchor for proper distribution of Pt particles which resulted as a superior catalytic activity for Pt-Re/TiO_2 even though the dispersion of Pt on ZrO_2 decreased by Re addition. According to the results of XPS, oxidation states between Re^{3+} and Re^{7+} contributed higher catalytic activity at Pt-Re/ZrO_2 than Pt/ZrO_2. Another study to understand the role of Re on WGS catalysts conducted by Choung *et al*. (2004). Re loading was the real reason behind the

proper dispersion of Pt on both catalysts ($Pt/Ce_{0.46}Zr_{0.54}O_2$, $Pt/Ce_{0.6}Ze_{0.4}O_2$) where it enhanced the activity of $Pt/Ce_{0.46}Zr_{0.54}O_2$ and $Pt/Ce_{0.6}Ze_{0.4}O_2$.

The objective of the study of Azzam *et al.* (2013) was to test the interaction of Re with $Pt\text{-}Re/TiO_2$. The reason behind the increment of water dissociation rate was reported as the reduction and oxidation cycle of ReO_x. According to the characterization methods, Re affected neither the Pt dispersion nor the surface area of TiO_2. The preparation without calcination and intermediary drying was held responsible for better activity and stability. The molar ratio of Pt/Re also played crucial role. Low ratio led decrement at active Pt sides where high ratio ensured high activity.

A kinetic study conducted to understand the real role of Re on Pt/TiO_2 by group of Azzam *et al*. (2008). Different reducible oxides supports (CeO_2, ZrO_2, TiO_2, $Ce_xZr_{1-x}O_2$ and $TixCe_{1-x}O_2$) were taking place with Pt-Re active metal-promoter combination. Kinetic research showed additional redox routes which were provided by the ReO_x sites for WGS reaction. Additional oxygen atom to CO to form CO_2 was given by ReO_x sites where ReO_x sites reoxidized with water to generate H_2. Due to the TPR studies, ReO_x was partially reduced at reaction conditions and still being available to provide oxygen for the reaction mechanism (Azzam *et al.*, 2008).

2.3.4. Vanadium Promoted Pt-based WGS Catalysts

A study carried out to understand the structures of vanadium on already studied successful catalyst Pt/CeO_2. It is known to present high oxygen mobility and has taken a large area of usage in the oxidation reactions. V in oxide form was taking the attention of researches to improve the activity and stability of Pt-based medium temperature WGS catalysts. (Farias *et al.*, 2008).

The wet impregnation and incipient to wetness impregnation techniques were used to prepare support and Pt-V impregnation, respectively. BET method was used to determine specific surface areas for prepared catalysts where V_2O_5 loading changed between 1-18 wt.%. In the light of BET measurement, V addition let a decrement in

surface area. According to XPS results, distribution of V^{5+}, V^{0}, V^{2+} and V^{3+}states on catalyst surface became wider when V loading was increased. Only V^{5+} oxidation states of V were observed when low V loadings with 1 wt.% were considered at $Pt/1VCeO_2$. In addition, formation of VOx species were favored more than polymeric or isolated species when V loading started to decrease. As the result of the situation explained above, distribution of Pt oxidation states strongly influenced from the presence of V.

X-ray diffraction method analysed $CeVO_4$ and V_2O_5 formations on the vanadium loaded $Pt/18VCeO_2$. These phases of V were illustrated with the high loading of vanadium. The creation of V^{5+}-O-Ce^{3+} sites correlated with the feature of vanadia to remove the oxygen from the most reducible surface oxides.

Among the prepared catalysts and the reaction temperature conditions between 200-350 °C, $Pt/6VCeO_2$ displayed the highest activity. Besides, V addition had positive effect on the activity of Pt/CeO_2. At $Pt/6VCeO_2$ catalyst configuration, formation of mono and polyvanadate species were examined by XRD and DRIFTS analyses. By the results of different spectroscopic techniques, V-O-V bonds caused activity drops and V-O-Ce bonds promoted the WGS reaction kinetics (Farias *et al.*, 2008).

In another research, Pt/ZrO_2 was promoted with different amounts of vanadia to observe the effect of V on the catalytic performance of Pt/ZrO_2. Activity tests were performed at 300 °C with realistic feed compositions (5.49% CO, 4.10% CO_2, 9.71% H_2, 49.95% N_2 and 30.75% H_2O). By the help of XRD, Raman and N_2 adsorption techniques appearance of vanadia was observed below monolayer coverage (monovanadate and polyvanadate) at the same time with V_2O_5 and ZrV_2O_7 species. Monovanadate that occurs at low vanadium loadings was held responsible for the superior activities. Results showed, monovanadate was primary contributer to the formation of V-O-Zr bounding on the surface of support. The most active catalyst was announced as 3 wt.% vanadia promoted catalyst which was three times more active than monometallic Pt/ZrO_2 (Thanh *et al*., 2008).

3. EXPERIMENTAL WORK

3.1. Materials

3.1.1. Chemicals

The solid and liquid chemicals used for catalyst preparation are listed in Table 3.1. All chemicals used are research grade.

Table 3.1. Chemicals used for catalyst preparation.

Chemical	Formula	Specification	Source	MW (g/mole)
Ammonium meta-vanadate	NH_4VO_3	99%	Riedel-de Haën	116.98
Ammonium perrhenate	NH_4ReO_4	99.999%	Sigma-Aldrich	268.24
Cerium (III) nitrate hexahydrate	$Ce(NO_3)_3.6H_2O$	99.99%	Sigma-Aldrich	434.23
Sodium carbonate	Na_2CO_3	99.9+%	Merck	105.99
Oxalic acid dihydrate	$C_2H_2O_4.2H_2O$	98%	Alfa Aesar	126.07
Tetraammineplatinum (II) nitrate	$Pt(NH_3)_4(NO_3)_2$	99.995%	Sigma-Aldrich	387.22
Water	H_2O	Deionized	-	18.02

3.1.2. Gases and Liquids

All of the gasses used in this study were supplied from Linde Group, Gebze, Turkey. Table 3.2 and 3.3 show the specifications and applications of the gases and liquids employed in this research, respectively.

Table 3.2. Specification and application of the liquid used

Liquid	Specification	Application
Water	Deionized (DI)	Aqueous solutions, Reactant

Table 3.3. Specifications and applications of the gases used.

Gas/Standard	Formula	Specification	Application
Argon	Ar	99.995%	Inert, Reducing agent, GC Carrier Gas
Carbon dioxide	CO_2	99.995%	Reactant, GC calibration
Carbon monoxide	CO	99.999%	Reactant, GC calibration
Dry air	N_2O_2 mixture	99.998%	GC 6-way pneumatic valve
Hydrogen	H_2	99.995%	Reactant, GC calibration
Methane	CH_4	99.995%	Reactant, GC calibration

3.2. Experimental Systems

The experimental systems used in this study can be divided into 3 main groups:

- Catalyst Preparation Systems: The system includes setups for support preparation (homogenous precipitation tech.) and incipient-to-wetness impregnation steps of catalyst preparation.
- Catalyst Characterization Systems: The techniques were used to analyze the structural properties of the prepared catalyst samples are included in this group of systems.

- Catalytic Reaction System: The system contains determining the catalytic activity, selectivity and stability. The feed section in continuous flow microreactor system included mass flow controller, HPLC pump and mixing zone; the reaction sections is including temperature controlled oven and an analysis section consists of gas chromatography that is connected to microreactor flow system for product analysis via gas chromatograms.

3.2.1. Catalyst Preparation System

The system used for catalyst preparation by incipient-to-wetness impregnation technique (Figure 3.1) includes a Retsch UR1 ultrasonic mixer, a vacuum pump, a büchner flask and a MasterFlex computerized-derive peristaltic pump.

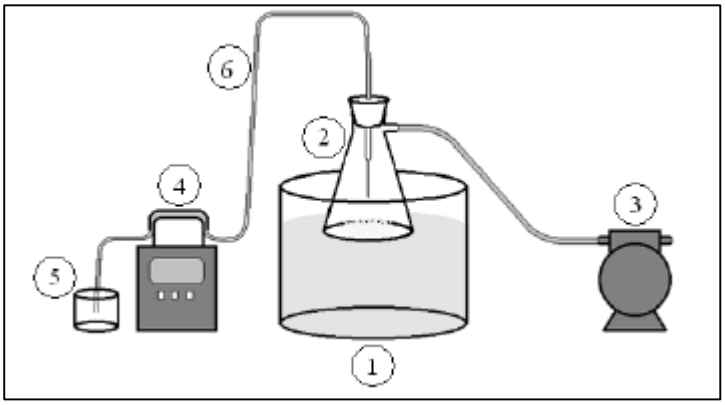

Figure 3.1. Schematic diagram of the impregnation system: 1. Ultrasonic mixer, 2. Büchner flask, 3. Vacuum pump, 4. Peristaltic pump, 5. Precursor solution beaker, 6. Silicone tubing (Demirhan, 2015).

The catalyst preparation process used in this study was divided into three steps:

- Evacuating the support
- Contacting support with prepared precursor solution
- Drying

The homogenous precipitation method used for support preparation (Figure 3.2). The system consists of a 400 ml beaker, a Julabo water bath, a Heidolph impeller and a Mettler Toledo pH-meter.

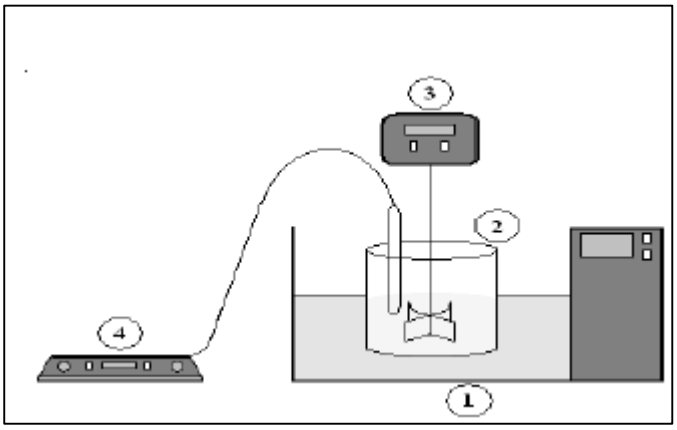

Figure 3.2. Schematic diagram of the homogenous precipitation system: 1. Water bath, 2. Beaker, 3. Impeller, 4. pH-meter (Demirhan, 2015).

3.2.2. Catalyst Characterization Systems

3.2.2.2. X-ray Photoelectron Spectroscopy (XPS). The oxidation states of the metallic species and the extent of electronic interaction between metal components present on the freshly reduced and used samples were investigated through determination the amounts of metallic phases by X-ray photoelectron spectroscopy (XPS). The analyses were performed at the Advanced Technologies Research and Development Center of Boğaziçi University with a K_α radiation source.

3.2.2.1. Raman Microscopy. The possible coke formations on the spend catalyst and the extents of V-O-Ce bond formation on the catalyst were examine with Raman spectroscopy. Raman spectra of the freshly reduced and spent catalysts were obtained by using a Renishaw inVia Raman microscope with the 514 nm 20 mW Ar^+ laser as the excitation per spectrum. The analyses were performed at the Advanced Technologies and Development Center of Boğaziçi University.

3.2.3. Catalytic Reaction System

The catalytic reaction system used in this study was designed and constructed in the Catalysis and Reaction Engineering Laboratory of Chemical Engineering Department (CATREL), Boğaziçi University. This system has three main parts: feed, reaction and product analysis.

The used reaction system originally designed with two consecutive reactors in order to enable testing the response of WGS catalyst performance, to the changes in OSR feed composition as in Figure 3.3. However, for this study, it was focused on the optimization of Pt-based trimetallic catalyst of WGS reaction, only the reactor 1 was used to perform reaction of WGS and GC 1 was used to analyze the gases.

The feed section was composed of mass flow control system (MFC), a high pressure liquid chromatography (HPLC) pump, 1/4'', 1/8'' and 1/16'' stainless steel (SS) tubing, valves and fittings for feed gaseous species, i.e. hydrogen, argon, carbon dioxide and carbon monoxide. The reactant high purity gases were supplied by pressurized cylinders that passing through pressure regulators at the pressure of 2.5 bar. The flow rates of the gasses were controlled by Brooks Instrument mass flow controller and the set values of the gasses were adjusted by Brooks Instrument 0154 series control box. On-off valves were placed in front of the mass flow controllers to protect them from possible back-pressure fluctuations. Each gas was fed from its independent line, in order to adjust desired feed composition and evaluated the flow of individual species.

The water introduction to the system at constant flow rates was provided by Jasco PU-2089 Plus quaternary gradient pump while the flow rates of the gases were controlled by Brooks Instrument mass flow controllers. The whole reactant mixing zone were kept at 130±5 °C while the water line had 1/16'' stainless steel tubing and to feed water in gaseous state, using a heating tape, a 16-gauge wire K-type fiberglass sheathed thermocouple and Shimaden SR91 temperature controller. The ceramic wool insulation was used to prevent heat losses from the heating tape. Reaction section was composed of 47 cm×20 cm×20 cm furnaces with 3.4 cm OD controlled by a Shimaden FP23

programmable temperature controller, 1/4'' OD stainless steel down-flow tubular microreactor that is 56 cm long and a K-type sheathed thermocouple. During the reaction tests, the catalyst bed was stabilized in the center of the microreactor by the silane based glass wool. Ceramic glass wool insulations were placed in top and bottom end or the furnace of the reactor to prevent heat loss and provide a stable temperature profile.

The product stream that leaves the reactor involves steam. Two cold traps were placed before GC inlet to condense water since steam is known as harmful material for gas chromatograph column.

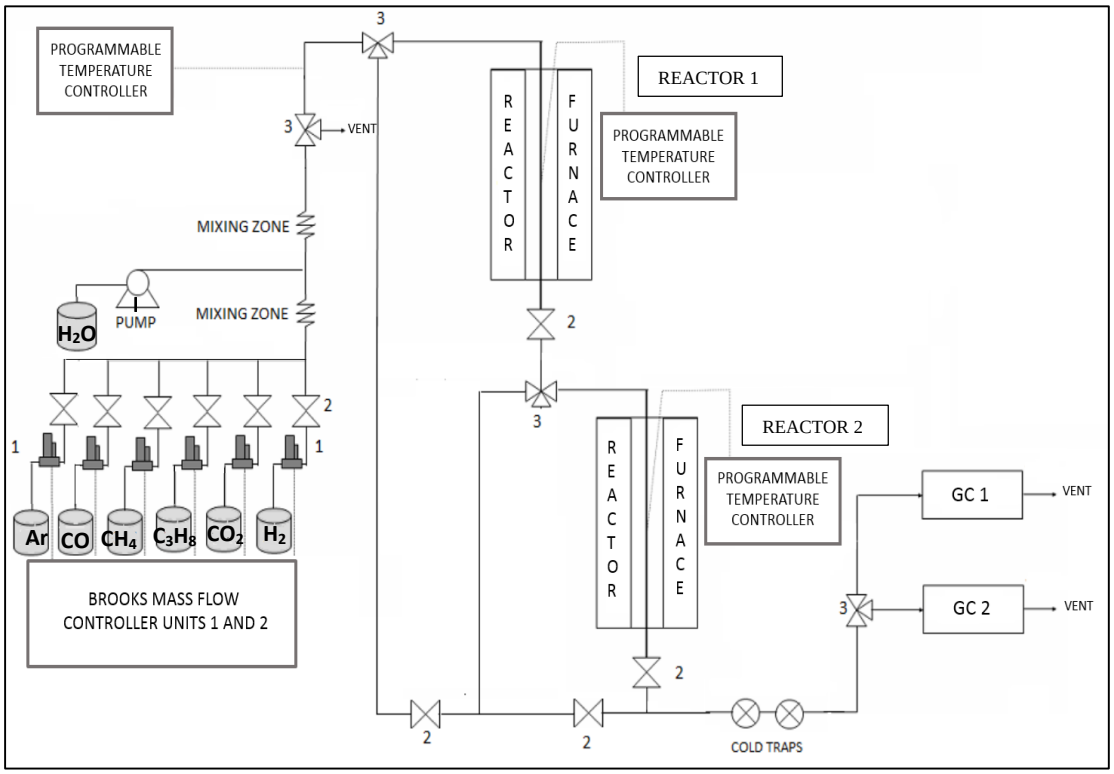

Figure 3.3. Schematic representation of the WGS reaction system: 1. Mass flow controller, 2. On-off valve, 3. Three-way valve (Gökaliler, 2012).

3.2.4. Product Analysis System

An Agilent Technologies 6850 gas chromatograph (GC) equipped with a Thermal Conductivity Detector (TCD) and a HayeSep D column was used to detect feed and dry product streams. Hourly time-on-stream (TOS) data was used to report the catalyst performance. Analysis conditions of the GC are given in Table 3.4 below.

Table 3.4. Gas analysing conditions for WGS analysis system.

GC Specifications	**Agilent Technologies 6850**
Carrier gas	Argon
Carrier gas flow rate (ml/min)	15.7
Column length & Inner diameter	2.54 m x 3 mm
Column temperature (°C)	40
Column packing material	Hayesep D
Column tubing	0.318 cm-Stainless steel
Detector temperature (°C)	150
Detector type	TCD
Gases analyzed	H_2, CO, CO_2
Inlet tempertature (°C)	100
Sample loop (ml)	1

GC was calibrated before proceeding with the experiments. Calibration was made by the injection of known values of gases under the given conditions in Table 3.4. In the preparation of the calibration curves, known volumes of gases were fed and peak areas were measured, then volume percent versus peak area curves were drawn and estimation factors were determined by linear regression.

3.3. Catalyst Preparation and Pretreatment

3.3.1. Preparation of Support

Figure 3.2 shows the support preparation. About 20 g of cerium (III) nitrate hexahydrate precursor was put in a beaker along with 100 ml of DI water to obtain pH 8 of the suspension at 60 °C water bath by homogenous precipitation technique. The desired pH was obtained by aqueous solution of sodium carbonate being the precipitation agent while continuously stirred with an impeller at a rate of 200 RPM. The slurry was left for an hour mixing after adjusting to willing pH under controlled temperature in a 60 °C water bath. A thoroughly stirred mixture was then filtered under vacuum by using Watman filter paper with number four and after the remnant was being washed with DI water the material was dried overnight at 110 °C in a drying oven and calcined in a muffle furnace at 400 °C for 4 hours.

3.3.2. Preparation of Catalyst Samples

V addition to CeO_2 support was applied by incipient-to-wetness impregnation technique described above in Figure 3.1. In this method determined amount of support was put in a büchner flask that stays in an ultrasonic mixer and kept under vacuum before and during the impregnation procedure. The support material was kept at ultrasonic mixer and under vacuum for 25 minutes to remove trapped air from pores of support to allow uniform distribution for the active components. Oxalic acid dehydrate was mixed with ammonium meta-vanadate to increase the solubility of ammonium meta-vanadate. The precursor solution containing the mixture of ammonium meta-vanadate and oxalic acid was applied with a 1:1.5 molar ratio in a defined amount of water (1.25 ml DI water/g support material). The prepared aqueous solution was impregnated on the support by using Masterlex computerized-derive peristaltic pump at a ratio of 0.5 ml/min. The resulting slurry was kept under 1.5 hours ultrasonically mixer, dried overnight at 115 °C and then calcined for 2 hours at 400 °C in a muffle furnace.

Re addition to V impregnated CeO_2 support was conducted via incipient-to-wetness impregnation technique. The aqueous solution of ammonium perrhenate was prepared by dissolving calculated amount of precursor salt in defined amount of water (1.1 ml DI water/g support material). The support was mixed ultrasonically 25 minutes before impregnating the aqueous solution. The prepared precursor solution impregnated at a rate of 0.5 ml/min by using Masterlex computerized-derive peristaltic pump on the ultrasonically mixed support. Re impregnated thick slurry was left under vacuum for 1.5 hours in order to obtain uniform distribution of metals on the vanadium impregnated ceria support. After 1.5 hours the prepared slurry was put in a 115 °C drying oven for an overnight, then calcined at 400 °C for 2 hours in a muffle furnace.

Pt addition to V-Re impregnated ceria support was performed with the dissolved tetraammineplatinum (II) nitrate salt ratio of 1.1 ml DI water for g ceria support material. A MasterFlex computerized-drive peristaltic pump was used for impregnation through silicone tubing with a rate of 0.5ml/min as explained at V and Re impregnation process. After impregnation procedure was applied, prepared slurry was kept under vacuum for more 1.5 hours; then dried overnight at 110 °C to remove water. The last calcination step after Pt impregnation was kept at 400 °C for 4 hours.

Table 3.5. List of Pt-Re-V/CeO_2 trimetallic WGS catalysts.

Catalyst Name	**Pt wt.%**	**Re wt.%**	**V wt.%**
0.5Pt-1Re-1V/CeO_2	0.5	1	1
1Pt-0.5Re-1V/CeO_2	1	0.5	1
0.5Pt-1Re-0.5V/CeO_2	0.5	1	0.5
1Pt-0.5Re-0.5V/CeO_2	1	0.5	0.5

3.3.3. Pretreatment Procedure of the Catalysts

Optimum reduction procedure was occurred for Pt-Re-V trimetallic WGS catalyst as 375 °C for 2 hours. The catalyst bed was heated from room temperature to 375 °C in 40 minutes under 15% hydrogen and 85% argon flow feed. After achieving desired

temperature, the catalyst samples were reduced *in situ* under same amount of gases for 2 hours.

3.4. WGS Performance Tests

The experiments with trimetallic Pt-Re-V/CeO_2 catalysts that specified in Table 3.5 were investigated at 300, 350 and 400 °C for two realistic feed compositions. The WGS reaction performance conducted over 75 mg freshly reduced catalyst sample. The total flow rate was 150 ml/min and the studies were conducted with the feed conditions listed in the Table 3.6. with 120,000 $mlg^{-1}h^{-1}$ GHSV. The feed composition was kept under 1.5 h mixing in order to get steady state gas compositions after the reduction of the catalyst sample. The catalyst was kept under Ar gas flow while the feed composition was mixed. The reaction tests were performed for 6 h time-on-stream (TOS). First product analysis were done 30 minutes after the connection of feed flow with freshly reduced catalyst. After making six more product analysis at every one hour; three feed analyses were performed. The reactions were carried out along with other specifications are presented in Table 3.7.

Table 3.6. List of feed compositions of WGS reaction used in this study.

Feed Name	**H_2O/CO Ratio**	**Flow Composition**
Feed #1	6.7	4.9% CO, 32.7% H_2O, 30% H_2, 10.4% CO_2, 22% Ar
Feed #2	16.2	2.1% CO, 34.1% H_2O, 23.7% H_2, 12.3% CO_2, 27.8% Ar

Table 3.7. List of the performed experiments in this study.

Catalyst	**H_2O/CO**	**Temperature (°C)**	**Experiment #**
0.5Pt-1Re-1V/CeO_2	16.2	350	1
	6.7	350	2
	6.7	400	3
	16.2	400	4
	16.2	300	5
	6.7	300	6
1Pt-0.5Re-1V/CeO_2	16.2	350	7
	6.7	350	8
	16.2	400	9
	6.7	400	10
	16.2	300	11
	6.7	300	12
0.5Pt-1Re-0.5V/CeO_2	16.2	350	13
	6.7	350	14
	16.2	300	15
	6.7	300	16
	16.2	400	17
	6.7	400	18
1Pt-0.5Re-0.5V/CeO_2	16.2	350	19
	6.7	350	20
	16.2	400	21
	6.7	400	22
	6.7	300	23
	16.2	300	24

4. RESULTS AND DISCUSSIONS

The aim of the current work is to design and develop Pt-based, CeO_2 supported trimetallic Pt-Re-V/CeO_2 catalysts(s) having high WGS activity, selectivity and stability with suppressed methanation under realistic feed *(i.e. feeds simulating typical reformer outlet)* flow in HTS-LTS transition temperature region, allowing the use of a single WGS reactor in fuel processors.

In this context, four Pt-Re-V/CeO_2 catalysts with different Pt, Re and V loadings, presented in Table 3.5, were developed, characterized and tested for their performances in WGS reaction. There, Re was used to modify the electronic structure of Pt, while V was added as a third metal/promoter aiming to benefit from the involvement of oxygen bridge formations, V-O-Ce and V-O-V, in WGS surface reaction. In the studies, catalyst composition (i.e. Pt:Re:V loading ratios), temperature (300, 350 and 400 °C) and H_2O/CO feed ratio in possible realistic feeds were used as the experimental parameters. Activity, selectivity, and stability of the catalyst samples were considered as the performance criteria. X-ray photoelectron spectroscopy (XPS) was used to analyze the oxidation states of the metals and support, and Raman spectroscopy was used to study the possible V-O-V and V-O-Ce bonds.

4.1. Water Gas Shift Performance Tests

WGS activity and stability characteristics of the catalysts prepared were investigated by using the experimental conditions listed in Table 3.7. For both realistic feeds, catalytic activity was reported as CO conversion level and/or amount of net H_2 produced. For comparing the activities of catalyst samples used in the experiments, 2 h TOS data were used (Figure 4.1 and 4.2). Blank tests were previously performed by Çağlayan (Çağlayan, 2011) showed the stainless steel reactor and CeO_2 support has no WGS activity for the reaction conditions used.

CO conversion level, as percentage of CO in the feed converted, and the net H_2 production, as net percentage increase in H_2 flow in product stream on the basis of that in the reactant stream, are evaluated by the Equation 4.1 and 4.2 respectively. The molar flow rate of each species in the feed and product streams is calculated by using Equation 4.3:

$$\text{CO conversion } (\%) = \left[\frac{F_{CO,in} - F_{CO,out}}{F_{CO,in}}\right] 100 \tag{4.1}$$

$$\text{Net } H_2 \text{ production } (\%) = \left[\frac{F_{H_2,out} - F_{H_2,in}}{F_{H_2,in}}\right] 100 \tag{4.2}$$

$$F_i \ (\mu\text{mol s}^{-1}) = \frac{P\, V_{i,gas}}{R\, T} \tag{4.3}$$

In Equation 4.3, P defines the atmospheric pressure, $V_{i,gas}$ is the volumetric flow rate of the gas, R is the universal gas constant and T is the absolute temperature.

CO conversion and the net H_2 and CO_2 production rates in $\mu\text{mol g}^{-1}\text{s}^{-1}$ are calculated by using Equation 4.4 and 4.5 respectively:

$$\text{CO conversion rate } (\mu\text{mol g}^{-1}\text{s}^{-1}) = \frac{F_{CO,in} - F_{CO,out}}{m_{cat}} \tag{4.4}$$

$$\text{Net gas production rate } (\mu\text{mol g}^{-1}\text{s}^{-1}) = \frac{F_{gas,out} - F_{gas,in}}{m_{cat}} \tag{4.5}$$

Percent loss of initial activity is used as the stability measure and is calculated by using Equation 4.6:

$$\text{Activity loss (\%)} = \left[\frac{(\text{CO conversion})_{0.5\text{h}} - (\text{CO conversion})_{6\text{h}}}{(\text{CO conversion})_{0.5\text{h}}}\right] 100 \qquad (4.6)$$

The full data obtained in TOS activity and stability tests are given in Appendix A.

4.1.1. Real Feed Tests

The performance tests were conducted under the flow of two realistic feeds over Pt-Re-V samples listed in Table 3.5. The feeds were chosen to simulate real reformer outlet having high and low H_2O/CO ratios, and their compositions are given in Table 3.6. Tests were performed under athmospheric pressure at three different temperature levels, 300, 350 and 400 °C. GHSV was kept at 120,000 ml g_{cat}^{-1} h^{-1} during the tests. Methane formation was not detected for any of the experimental conditions, which shows the catalysts tested suppressed secondary methanation activity during the performance tests.

Figures 4.1(a) and 4.1(b) display the temperature dependence of CO conversion and the net H_2 production, respectively, for a realistic feed composition, real feed #1 having H_2O/CO=6.7, at three different reaction temperatures used. Figure 4.1 additionally includes the thermodynamic equilibrium conversion profile that was calculated by HSC-Chemistry Software.

Results show that CO conversion activities are comparatively lower at 300 °C. The highest CO conversion levels were obtained over 1Pt-0.5Re-1V/CeO_2 and 1Pt-0.5Re-0.5V/CeO_2 at mid-temperature, i.e. 350 °C; for those samples CO conversion reached ca. 68% and ca. 71%, respectively. The net additionally produced H_2 was achieved as 12% at 350 °C meaning ca. 30.2 μmol/s hydrogen was produced over both catalyst samples. Parallel to the decrease in thermodynamic equilibrium conversion with temperature, 1Pt-0.5Re-1V/CeO_2 at 400 °C yielded lower CO conversion level (61.8%) and net H_2 production (11%) than the values obtained at 350 °C. The lowest CO conversion level (49.7%) and the net H_2 production (6.4%) was observed at 400 °C over 1Pt-0.5Re-0.5V/CeO_2 though this catalyst showed higher activity and net hydrogen production at

300 °C compared to those obtained over 1Pt-0.5Re-1V/CeO_2. Although CO conversion level increased from 44% to 58.2% in response to temperature rise from 350 to 400 °C over 0.5Pt-1Re-0.5V/CeO_2, a decrease in the net H_2 production from 8.3% to 6.8% was observed with temperature rise. The lowest hydrogen production rate (2%) among four samples for the given temperature range was obtained over 0.5Pt-1Re-0.5V/CeO_2 at 300 °C accompanied by a low CO conversion level ca.8.0%, which is just slightly below the conversion, ca. 8.5%, obtained over 0.5Pt-1Re-1V/CeO_2. It should be noted that, activity and net H_2 production over 0.5Pt-1Re-1V/CeO_2 dramatically increased in response to temperature rise. In general, except at 300 °C, CO conversion levels were not far below the equilibrium conversions for all samples, especially for 0.5Pt-1Re-0.5V/CeO_2 and 0.5Pt-1Re-1V/CeO_2 at 350 °C.

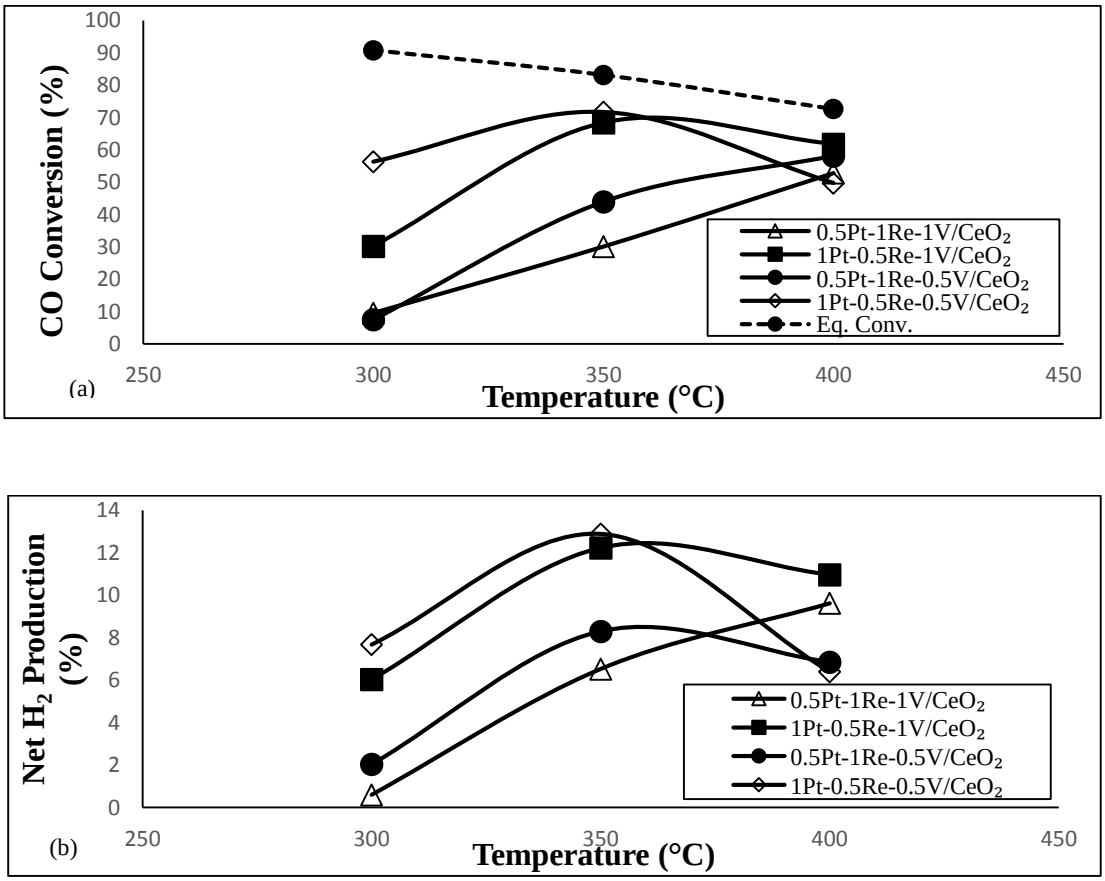

Figure 4.1. Temperature dependence of (a) catalytic activity and (b) net H_2 production for real feed #1, H_2O/CO = 6.7 (4.9% CO, 32.7% H_2O, 30.0% H_2, 10.4% CO_2, 22.0% Ar).

Figures 4.2(a) and 4.2(b) clearly illustrate the temperature dependence of both CO conversion and net H_2 production, respectively, for water-rich realistic feed (real feed #2; H_2O/CO= 16.2). Figure 4.2(a) additionally involves the equilibrium conversion calculated by HSC-Chemistry Software. Changing feed composition from real feed #1 to real feed #2, i.e. making feed richer in water through increasing H_2O/CO feed ratio, resulted in comparable activities on 1Pt-0.5Re-0.5V/CeO_2. However, for the other three catalysts, increasing H_2O/CO ratio of the feed led to a better performance at 300 °C, whereas to a decrease in CO conversion at 400 °C. Furthermore, this change in the feed stream resulted in a decrease in the net H_2 production values for all catalysts.

Over all the catalysts, except 0.5Pt-1Re-0.5V/CeO_2, CO conversion makes peak at 350 ^oC. Results showed that 1Pt-0.5Re-0.5V/CeO_2 has the highest CO conversion level, 73.4%, reaching almost equilibrium level, and net H_2 production rate, 7.1%, as well at 350 °C among the catalysts tested. Its CO conversion still remained very close to equilibrium at 400 ^oC. Similarly, CO conversion makes a peak, ca. 59%, at 350 °C over 1Pt-0.5Re-1V/CeO_2 and decreases down to ca. 49% at 400 ^oC. The net H_2 production over this catalyst reached its peak value as 6.2 % at 350 ^oC. Almost the same CO conversion levels were obtained over 1Pt-0.5Re-1V/CeO_2 and 0.5Pt-1Re-0.5V/ CeO_2 at 400 °C. However, 0.5Pt-1Re-0.5V/CeO_2 showed a continuous rise in both CO activity and net H_2 production with the increase in temperature for 300-400 ^oC range, probably owing to significantly lower-than-equilibrium CO conversion over the sample at 300 and 350 ^oC. 0.5Pt-1Re-1V/CeO_2 and 0.5Pt-1Re-0.5V/CeO_2 showed comparable activity-temperature relation, except the slight decrease observed for the temperature rise from 350 to 400 ^oC over 0.5Pt-1Re-1V/CeO_2. Net H_2 production is lower over 0.5Pt-1Re-1V/CeO_2 compared to that over 0.5Pt-1Re-0.5V/CeO_2 at temperatures greater than 300 °C.

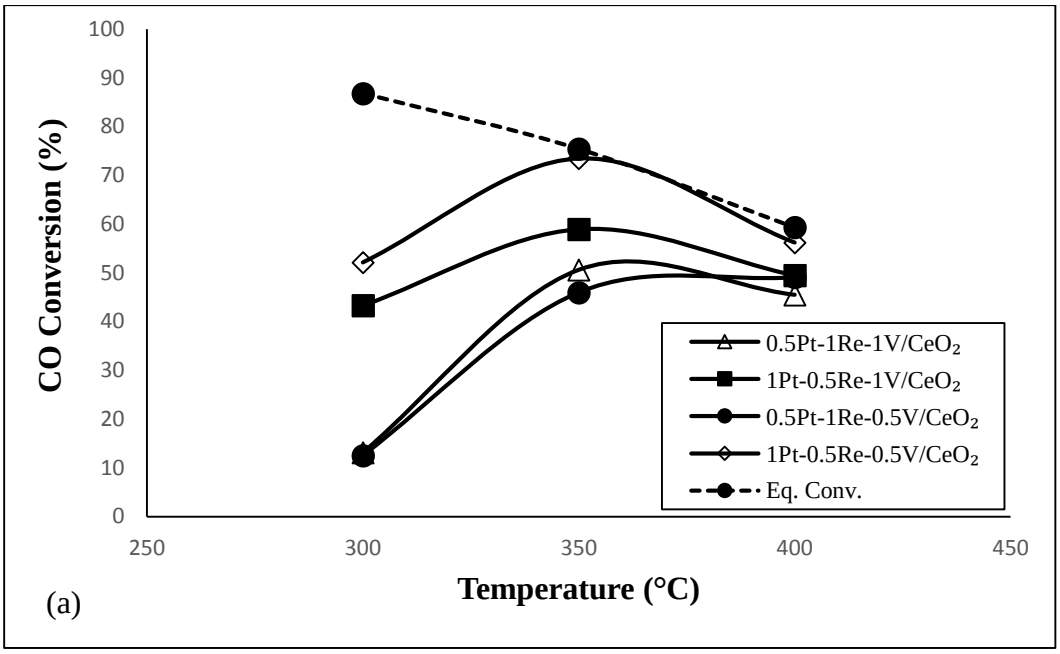

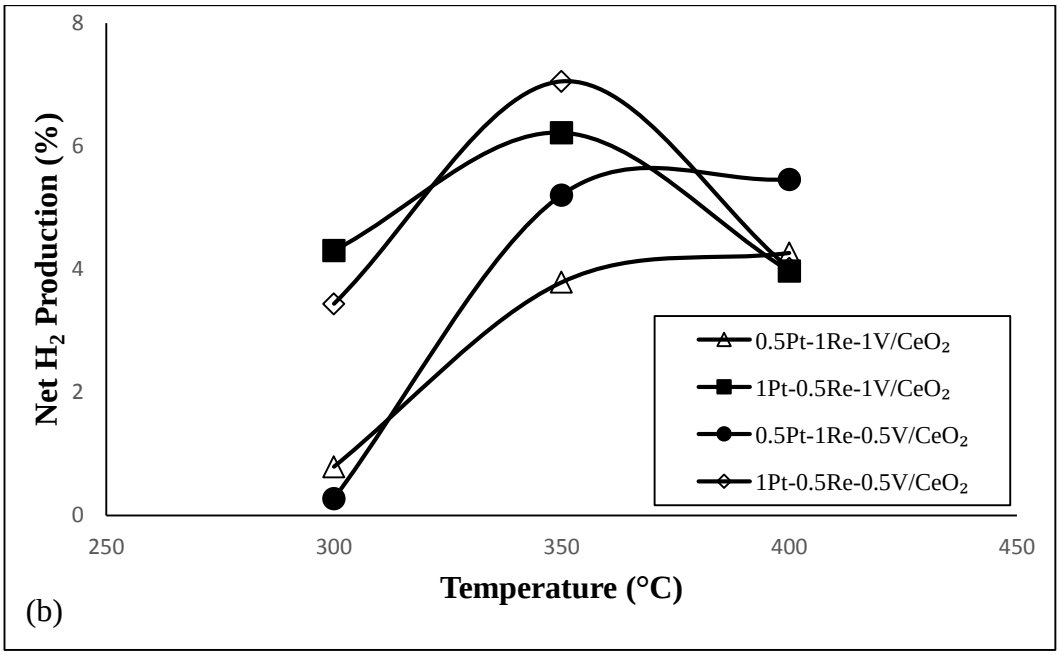

Figure 4.2. Temperature dependence of (a) catalytic activity and (b) net H_2 production for real feed # 2, H_2O/CO = 16.2 (2.1% CO, 34.1% H_2O, 23.7% H_2, 12.3% CO_2, 27.8% Ar).

Time dependent activity losses of the catalysts till the end of 6h TOS, representing the level of stability on the basis of initial activity at 30 min TOS, were calculated and illustrated in Figure 4.3 for real feed #1 at 350 °C. The catalysts showed superior activity, 1Pt-0.5Re-1V/CeO_2 and 1Pt-0.5Re-0.5V/CeO_2, with starting conversion levels just above 70% and comparable net H_2 production rates ca.12%, experienced 7.4% and 11.5% activity losses, respectively. It should be noted that between those, 1Pt-0.5Re-1V/CeO_2 had all its activity loss for the first 2h TOS and then its activity almost completely stabilized. The superior performance stability was obtained over 0.5Pt-1Re-0.5V/CeO_2 where the activity loss was only around 3%. Even though 0.5Pt-1Re-1V/CeO_2 had also superior stability, its CO conversion and net H_2 production values are the lowest between those of all the samples tested.

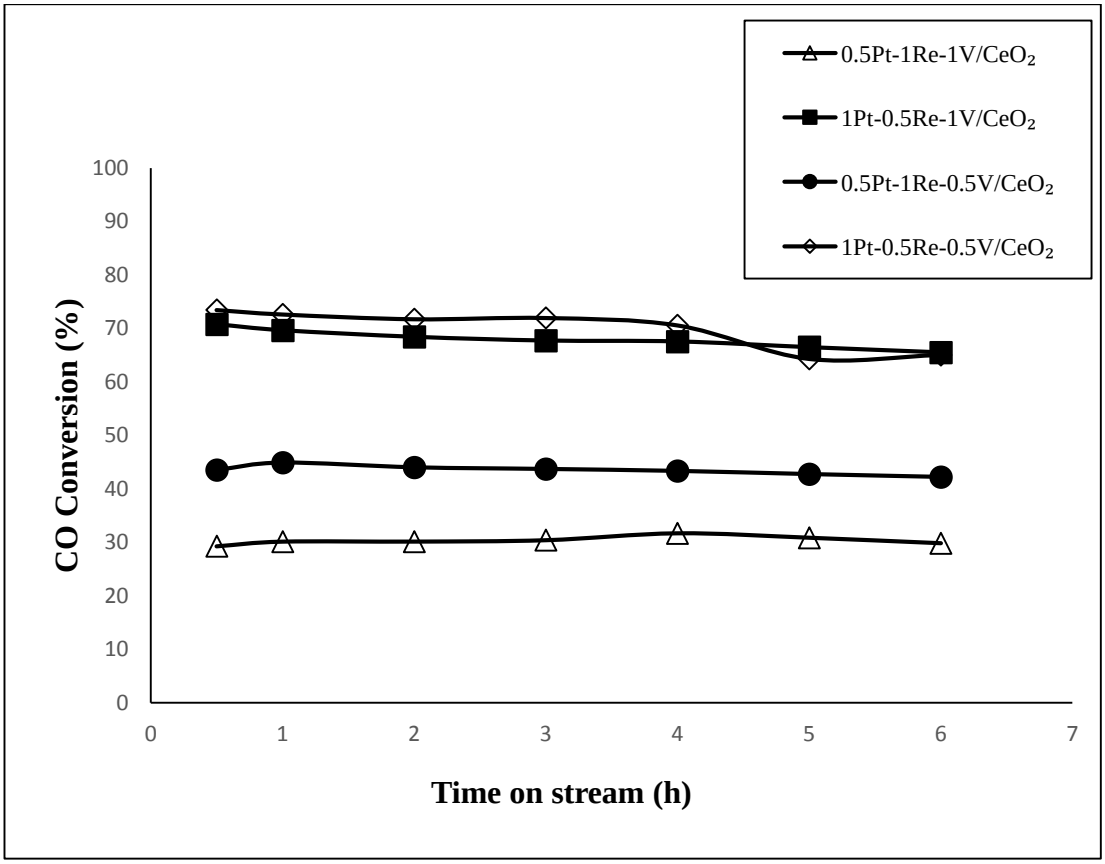

Figure 4.3. Stability values of studied catalysts for real feed #1, $H_2O/CO = 6.7$ at 350 °C (4.9% CO, 32.7% H_2O, 30.0% H_2, 10.4% CO_2, 22.0% Ar).

The activity losses of the catalysts till the end of 6h TOS on the basis of initial activity at 30 min TOS were calculated and illustrated in Figure 4.4 under the flow of real feed #1 at 400 °C. With the increase in temperature to 400 °C, comparable net H_2 production levels with an increase in the catalytic activity were observed over 0.5Pt-1Re-1V/CeO_2 and 0.5Pt-1Re-0.5V/CeO_2 compared to those at 350 °C. The lowest activity loss, ca.3.5%, was observed over 1Pt-0.5Re-1V/CeO_2; the CO conversion level decreased from ca. 62% at 30 min TOS to 60% at the end of 6 h TOS. The activity loss limited to ca. 5% for 0.5Pt-1Re-0.5V/CeO_2; the CO conversion level decreased from ca. 59% at 30 min TOS to 56% at the end of 6 h TOS. The activity loss increased and CO conversion level decreased for 1Pt-0.5Re-0.5V/CeO_2 with an increase in the reaction temperature from 350 to 400 °C.

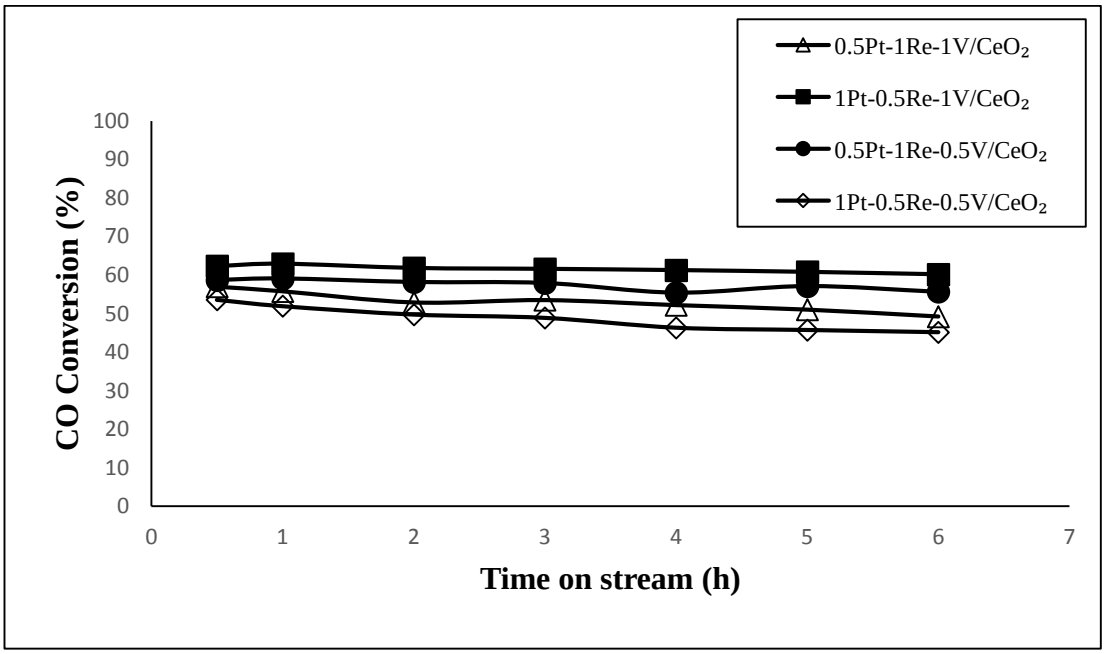

Figure 4.4. Stability values of studied catalysts for real feed #1, H_2O/CO = 6.7 at 400 °C (4.9% CO, 32.7% H_2O, 30.0% H_2, 10.4% CO_2, 22.0% Ar).

Comparative analysis of the results indicated that more stable activities were obtained for the whole temperature range, 300-400 °C, when real feed #2, which has higher H_2O/CO ratio, was used (not shown); the activity loss measured during the tests

under the flow of real feed #2 was at most 12% over all the catalysts tested. Activity loss data additionally revealed that rise in temperature from 350 to 400 ^{o}C resulted in greater stability for the two high performance catalysts, i.e. 1Pt-0.5Re-0.5V/CeO_2 and 1Pt-0.5Re-1V/CeO_2, when feed with high H_2O/CO ratio was used.

Real feed #1 and #2 contain almost the same concentrations of H_2, CO_2 and H_2O; the main difference between the feeds comes from the CO flows, which are 7.4 and 3.2 ml/min for real feed #1 and #2, respectively. In terms of net H_2 production values, real feed #1 which has less amount of CO yields greater net H_2 production values. Consequently, the results hint that limitation in CO amount in feed #2 may be the reason of lower net H_2 production.

In addition to catalytic activity and stability, net hydrogen production, which defines selectivity, is the third primary perfomance criteria of a succesful WGS catalyst. High selectivity is crucial since the goal of WGS unit of a fuel processor is decreasing CO concentration of the OSR outlet while increasing its H_2 concentration aiming to ease the workload of the following PROX reactor. The catalysts tested in the current study are not prone to methanation, which is considered as a detrimental side reaction causing hydrogen consuption during WGS. Figure 4.5 and 4.6 focus on the selectivity of four catalysts at 300, 350 and 400 °C for real feed #1 and #2, respectively. The rates measured at 6 h TOS are presented in both figures. The data presented in both figures clearly revealed that both catayst composition and reaction condition have strong effects on catalyst performance. Though there are exceptions, the catalysts reached their highest performance at 350 ^{o}C, most probably due to suppression of CO conversion due to lower themodynamic equilibrium at 400 ^{o}C. The highest net hydrogen production rates were observed over 1Pt-0.5Re-1V and 1Pt-0.5Re-0.5V samples for H_2O/CO poor and rich feed streams, respectively. It should be noted that the difference in the performance of those sample is rather small for low H_2O/CO feed ratio, while it becomes more significant, especially in CO conversion aspect, when H_2O/CO feed ratio is high. Another improtant finding is the importance of Pt in WGS performance; both 0.5% Pt loaded samples have inferior performance under the flow of both feeds. In general, those findings confirm crucial role of Pt-Re interaction in H_2O activation, and hints that when

Re:V ratio is low, the contribution of Re to performance in water rich conditions is suppressed.

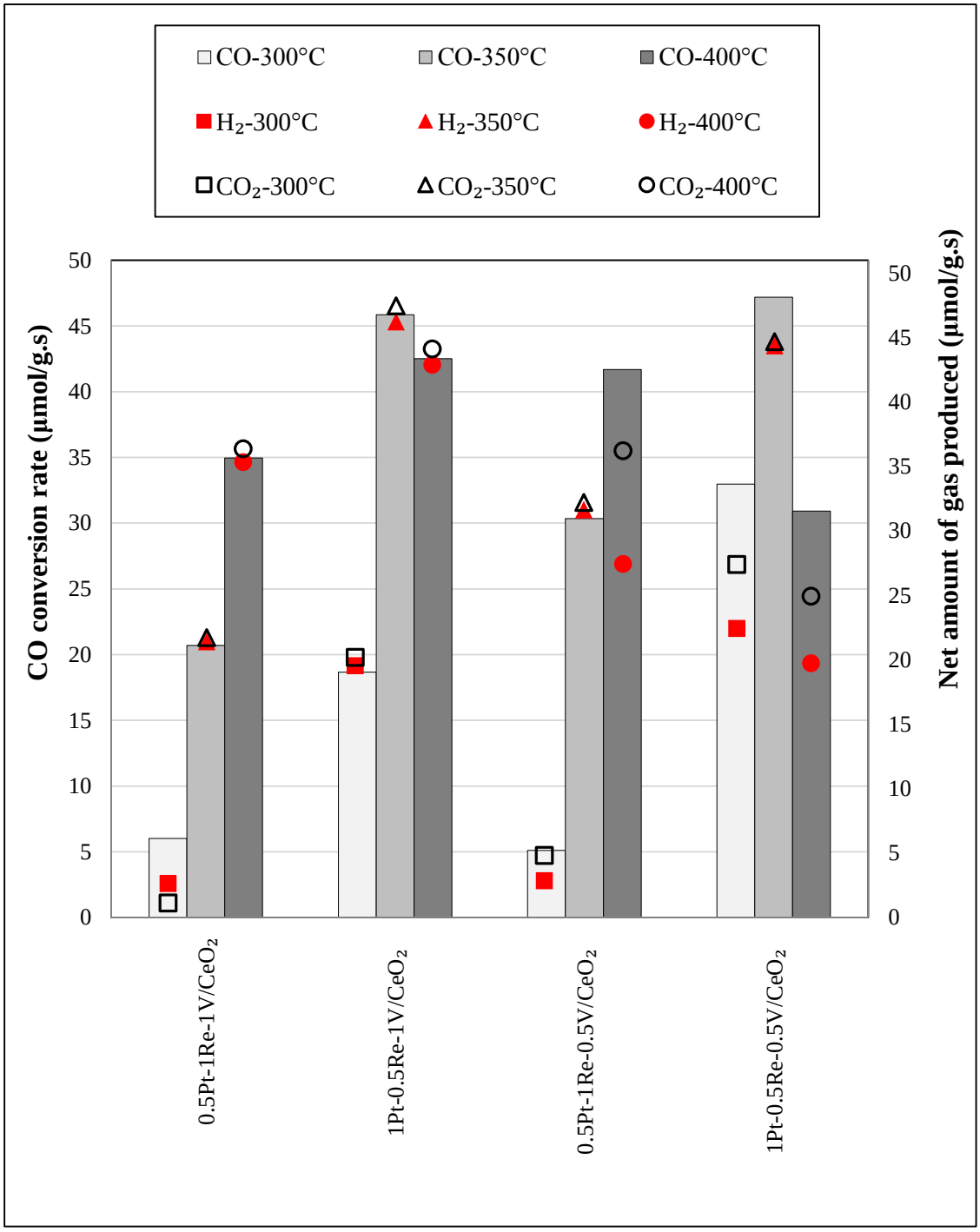

Figure 4.5. Effects of catalyst on the CO conversion and the net H_2, CO_2 production rates for real feed #1 (H_2O/CO = 6.7) at the end of 6 h TOS.

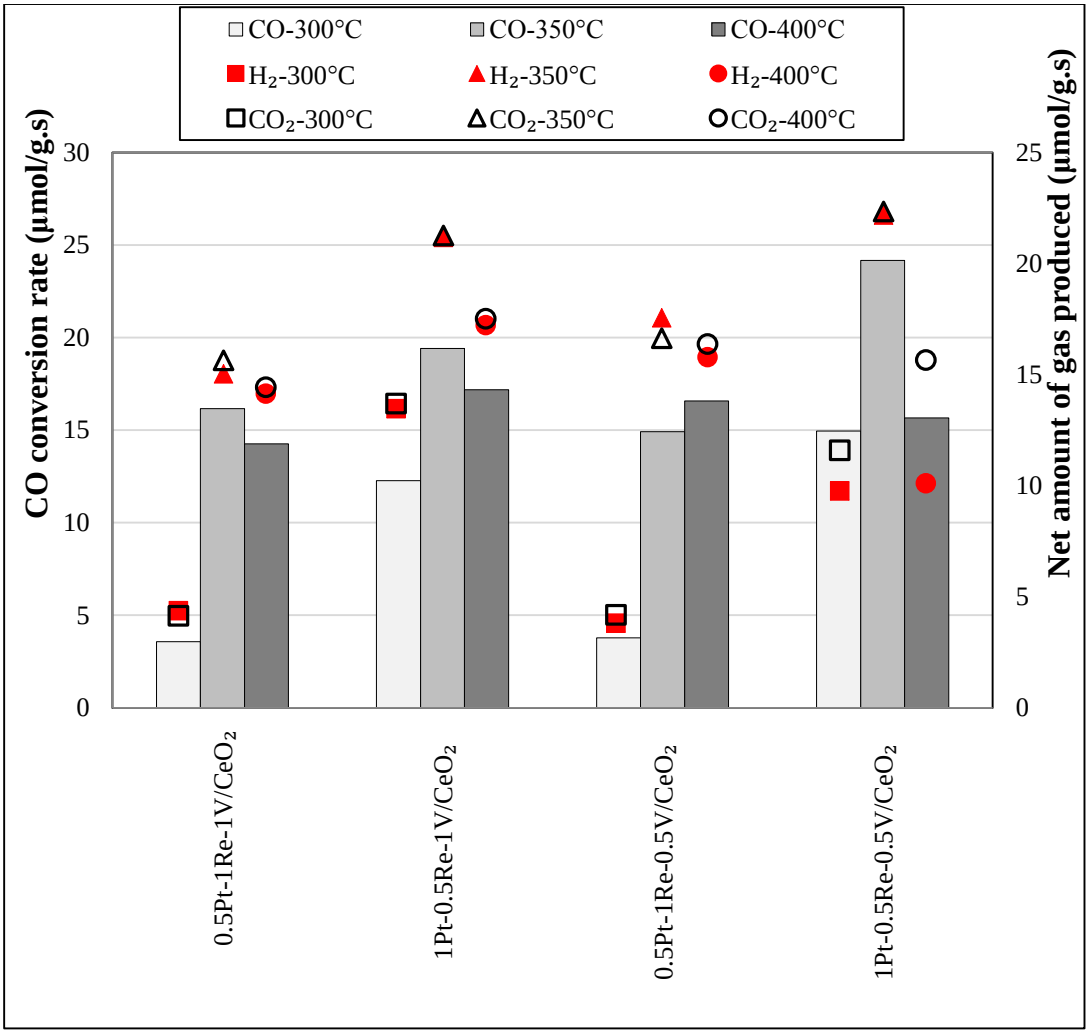

Figure 4.6. Effects of catalyst on the CO conversion and the net H_2, CO_2 production rates for real feed #2 (H_2O/CO = 16.2) at the end of 6 h TOS.

The CO conversion levels reached in all performance tests, which are presented in Figure 4.7, clearly illustrate a 'CO conversion-temperature' trend. CO conversion values are the highest over high performance samples, 1Pt-0.5Re-1V/CeO_2 and 1Pt-0.5Re-0.5V/CeO_2, at 350 °C as their CO conversion values are very close to that of the equilibrium, while the conversion levels decrease, parallel to the decrease in equilibrium conversion, with increase in temperature to 400 °C. On the other hand, as the samples with inferior performance, 0.5Pt-1Re-1V/CeO_2 and 0.5Pt-1Re-0.5V/CeO_2, have CO

conversion values far below equilibrium at 350 ºC, there is an increase observed in their CO conversion as the temperature is risen to 400 °C.

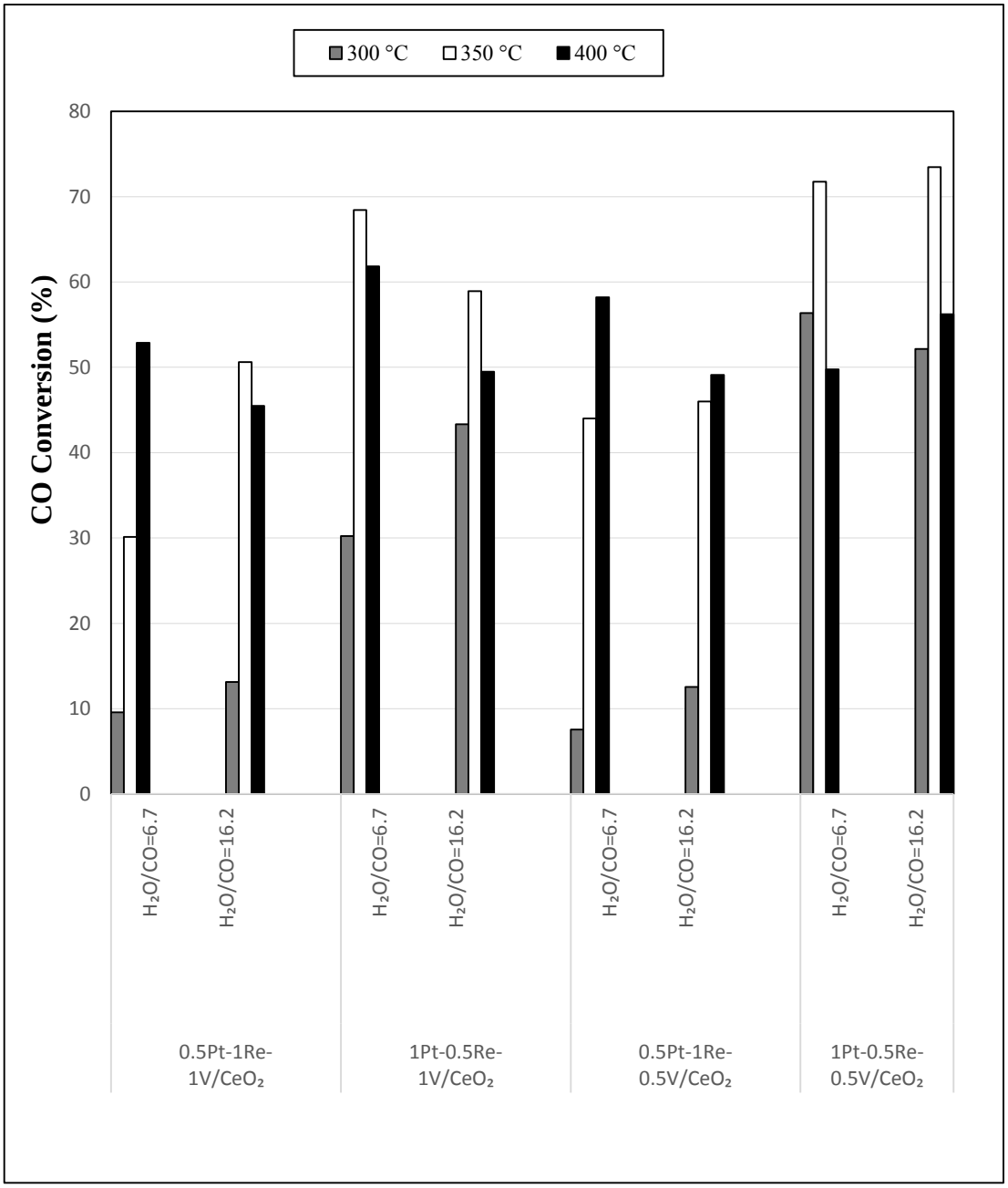

Figure 4.7. Temperature dependence of catalytic activities for four catalysts in real feed #1 and #2.

In general, the results revealed that 1Pt-0.5Re-1V/CeO_2 and 1Pt-0.5Re-0.5V/CeO_2 have great potentials to be used in a fuel processor as a WGS catalyst owing to their high activity, stability and selectivity. Another important point is that those catalysts can make the use of a single stage WGS unit in an FP possible instead of conventional two stage (HTS and LTS) WGS unit.

4.2. Catalyst Characterization

4.2.1. XPS

Oxidation states and elemental compositions of the metallic species present on the surface of catalysts were investigated by X-ray photoelectron spectroscopy (XPS). XPS is an important method to study both the changes on the surface upon reaction and the distribution of the metallic and oxide phases when the catalyst composition is changed. The characteristic oxidation states of Ce, O, V, Re and Pt atoms were shown by the XP spectra of freshly reduced and spent catalyst samples.

Ce 3d XP spectra of freshly reduced Pt-Re-V/CeO_2 catalysts are displayed in Figure 4.8, in which the principal spin-orbit state peaks for Ce $3d_{3/2}$ and Ce $3d_{5/2}$, indicating Ce^{3+} and Ce^{4+} oxidation states, are labeled as v and u respectively. The XP spectra of Ce 3d region of all catalyst samples studied were in accordance with the literature (Leppelt *et al.*, 2006; Çağlayan and Aksoylu, 2011). The slight red and blue shifts of the Ce 3d spectra of the freshly reduced catalyst samples can be attributed to the incorporation of the metals of the trimetallic catalyst into the ceria lattice (Çağlayan and Aksoylu, 2011) and the variance in composition of the freshly reduced catalyst samples.

The detailed analysis of Ce oxidation states is an important parameter considering the redox properties of CeO_x. After the deconvolution of the spectra via Avantage software, the degree of ceria reduction was evaluated from the ratio of the sum of the corresponding integrated peak areas by the formula given below (Çağlayan and Aksoylu 2011, Leppelt *et al*., 2006):

$$[Ce^{3+}] = I - Ce^{3+}/(I - Ce^{3+} + I - Ce^{4+})$$

where, $I - Ce^{3+}$ and $I - Ce^{4+}$ represent the sum of the intensities of two doublets resulting from Ce_2O_3 and three doublets resulting from CeO_2, respectively.

The amount of Ce^{3+} present on the freshly reduced 0.5Pt-1Re-0.5V/CeO_2, 0.5Pt-1Re-1V/CeO_2, 1Pt-0.5Re-0.5V/CeO_2 and 1Pt-0.5Re-1V/CeO_2 catalysts were estimated as 21.1, 18.0, 17.7 and 22.2%, respectively.

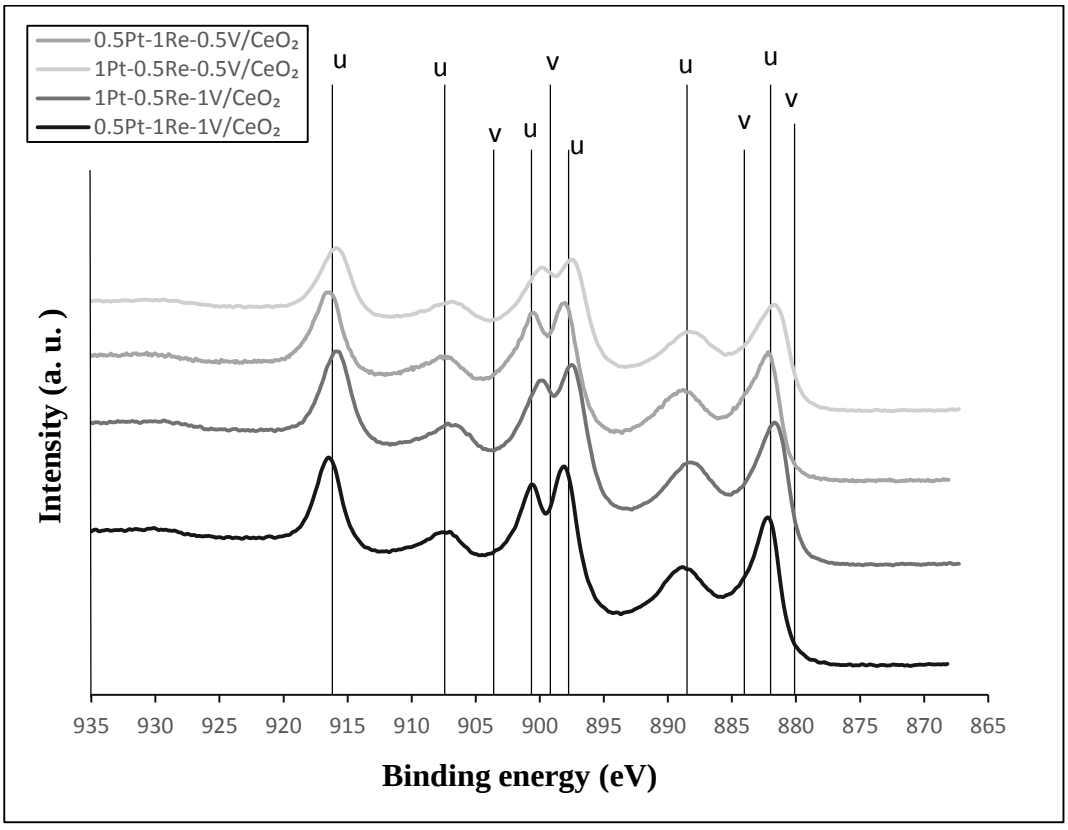

Figure 4.8. Ce 3d XP spectra of freshly reduced catalyst samples (v: Ce^{3+}, u: Ce^{4+}).

Vanadium oxides are well known and studied for their redox properties (Bautista *et al.,* 2006, Boyesen *et al.,* 2015, Haber *et al.,* 1986). The Ce 3d XP spectra of freshly reduced and spent 1Pt-0.5Re-0.5V/CeO_2 and 1Pt-0.5Re-1V/CeO_2 samples are compared in Figure 4.9 in order to understand the effect of V-loading on Ce oxidation states

through possible Ce-V interaction. The Ce 3d XP spectra of freshly reduced and spent 0.5Pt-1Re-1V/CeO_2 are also given considering the catalyst's high performance during the reaction tests. WGS experiments were conducted at 350 °C during 6 h TOS under real feed flow with H_2O/CO ratio of 16.2 to obtain the spent catalyst samples. The resulting spectra indicated that the peaks showing Ce^{3+} and Ce^{4+} were observed on fresh and spent catalyst samples however the peak intensities were lower for the spent forms of catalysts. In addition, peaks belonging to all spent catalyst samples were observed to have a shift to lower binding energies when compared to the peaks from the freshly reduced catalyst samples. This shift was clearly observed for 1Pt-0.5Re-0.5V/CeO_2 catalyst.

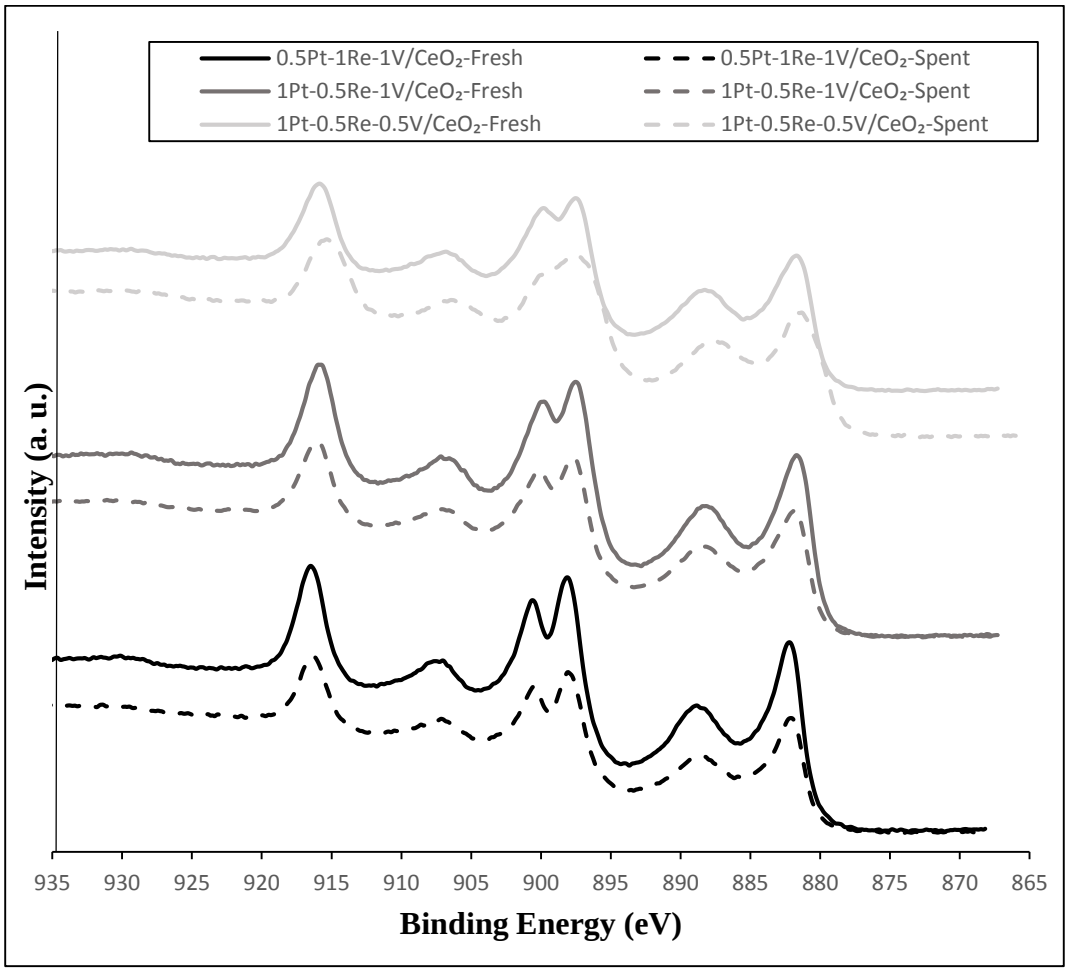

Figure 4.9. Ce 3d XP spectra of freshly reduced and spent catalyst samples.

The Ce^{3+} contents of the freshly reduced and spent catalyst samples are presented in Table 4.1. Since Ce^{3+} plays a crucial role in increasing electron transfer ability from the support to metallic sites (Tabakova *et al*., 2003; Çağlayan and Aksoylu, 2011), and Ce^{3+} ions are highly active towards reactants due to excess electrons that are left behind when an oxygen atom is removed (Campbell and Peden, 2005), Ce^{3+} content is reported to be slightly higher in the case of the catalysts with higher WGS activity. As a result of the electron transfer during reaction, the amount of Ce^{3+} is expected to decrease for the catalyst samples upon reaction. Accordingly, the % decrease in the Ce^{3+} content for the better performing 1Pt-0.5Re-1V/CeO_2 was calculated as 22.1. The increase in the Ce^{3+} content for 1Pt-0.5Re-0.5V/CeO_2 catalyst sample after reaction was considered as an experimental error.

In order to find a correlation between the WGS activity of 1Pt-0.5Re-1V/CeO_2 and its Ce^{3+} percentage, the Ce 3d XP spectra of the catalyst tested under two different real feed conditions – namely, real feed #1: H_2O/CO=6.7, 350 °C, (4.9% CO, 32.7% H_2O, 30.0% H_2, 10.4% CO_2, 22.0% Ar) and real feed #2: H_2O/CO=16.2, 350 °C, (2.1% CO, 34.1% H_2O, 23.7% H_2, 12.3% CO_2, 27.8% Ar) - were compared. Figure 4.10 and Table 4.2 represent the Ce3d XP spectra and the Ce^{3+} content of freshly reduced and spent 1Pt-0.5Re-1V/CeO_2 catalyst samples, respectively. The comparative analysis of the Ce 3d spectra (Figure 4.10) show a slight decrease in the intencities of the spectra obtained for the spent samples. This change is also valid for the spent species of 0.5Pt-1Re-1V/CeO_2, 0.5Pt-1Re-0.5V/CeO_2 and 1Pt-0.5Re-0.5V/CeO_2 (not shown). As explained above, calculated Ce^{3+} content on the surface of the spent forms of 1Pt-0.5Re-0.5V/CeO_2 catalyst were expected to decrease as a result of the crucial role of Ce^{3+} ions during reaction (Table 4.2). The reaction under real feed #2 conditions with high H_2O/CO feed ratio resulted in lower Ce^{3+} percentage compared to that obtained with real feed #1. Although the higher net decrease in the Ce^{3+} content was not obtained for the sample which was tested under conditions resulting higher net H_2 production, it should be kept in mind that, for 1Pt-0.5Re-1V/CeO_2 catalyst, WGS reaction under both conditions resulted in comparable CO conversion values (~75%); this value being very close to the equilibrium value for the conditions with the higher H_2O/CO feed ratio.

Table 4.1. Ce^{3+} contents (%) of the freshly reduced and spent catalyst samples (Real feed #2, H_2O/CO=16.2; 350 °C; 2.1% CO, 34.1% H_2O, 23.7% H_2, 12.3% CO_2, 27.8% Ar).

Catalyst	**Ce^{3+} (%)**	
	Freshly reduced	**Spent**
0.5Pt-1Re-1V/CeO_2	18.0	15.6
1Pt-0.5Re-1V/CeO_2	22.2	17.3
0.5Pt-1Re-0.5V/CeO_2	21.1	20.5
1Pt-0.5Re-0.5V/CeO_2	17.7	19.7

Table 4.2. Ce^{3+} content (%) of 1Pt-0.5Re-1V/CeO_2 freshly reduced and spent samples for two different feed conditions.

Catalyst	**Ce^{3+} (%)**	
	Freshly reduced	**Spent**
RF #1 – 350 °C	22.2	18.55
RF #2 – 350 °C	22.2	17.3

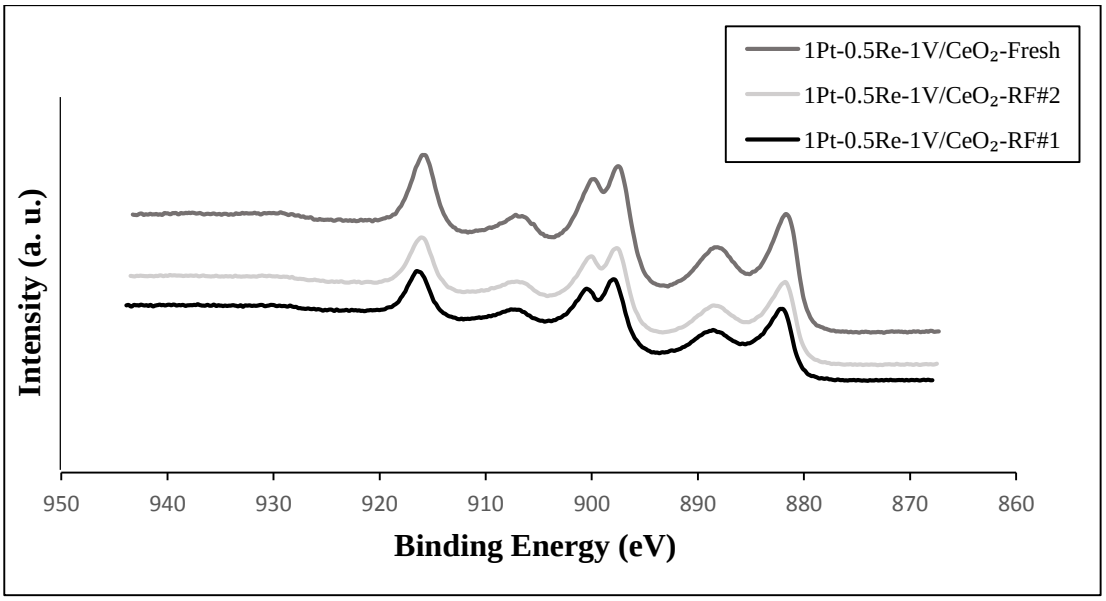

Figure 4.10. Ce 3d XP spectra of freshly reduced and spent catalyst samples tested under two different real feed conditions at 350 °C.

Figure 4.11 illustrates the V 2p XP spectra of the freshly reduced and spent 0.5Pt-1Re-1V/CeO_2, 1Pt-0.5Re-0.5V/CeO_2 and 1Pt-0.5Re-1V/CeO_2 catalyst samples. The peak at 516.5 eV, corresponding to the V^{4+}oxidation states (Suchorski *et al*., 2005, Duarte de Farias *et al*., 2008) can be assigned to V^{4+} ions of the VO_2 compound, which has been reported to have promotion effect in the WGS activity (Demeter *et al*., 2000-Silversmit *et al*., 2004-Junior *et. al*., 2005). This band's direct relation to WGS activity can be clearly seen from Figure 4.11; V 2p XP spectrum of the freshly reduced 1Pt-0.5Re-1V/CeO_2 catalyst, which has the highest WGS activity among the catalysts has the highest area for the 516.5 eV band. While VO_2 containing V^{4+} ions are accepted to be the active compound for the WGS reaction, V_2O_5 is reported to be inactive. V^{5+} ions are attributed mainly to V_2O_5 compounds, which are reported to be inactive in WGS reaction mostly due to the presence of V–O–V bonds (Ballarini *et al*., 2006-Duarte de Farias *et al*., 2008). It should be noted no peaks belonging to the V^{5+} phase (~523 eV) were observed in any of the V 2p spectra of the catalysts tested. 515 eV band, which can be clearly observed on the spectra of the spent forms of the 0.5Pt-1Re-1V/CeO_2 and 1Pt-0.5Re-1V/CeO_2 catalyst samples, is attributed to V^{3+} species. The mentioned band was reported to emerge as the V loading of 1Au-0.5Re-1V/CeO_2 and Pt-V/CeO catalysts were increased (Demirhan 2015, Duarte de Farias *et al.*, 2008). In our case, V^{3+} species were formed during reaction and/or their surface concentration increased as the active V^{4+} components were involved in the WGS reaction for 1% V catalysts.

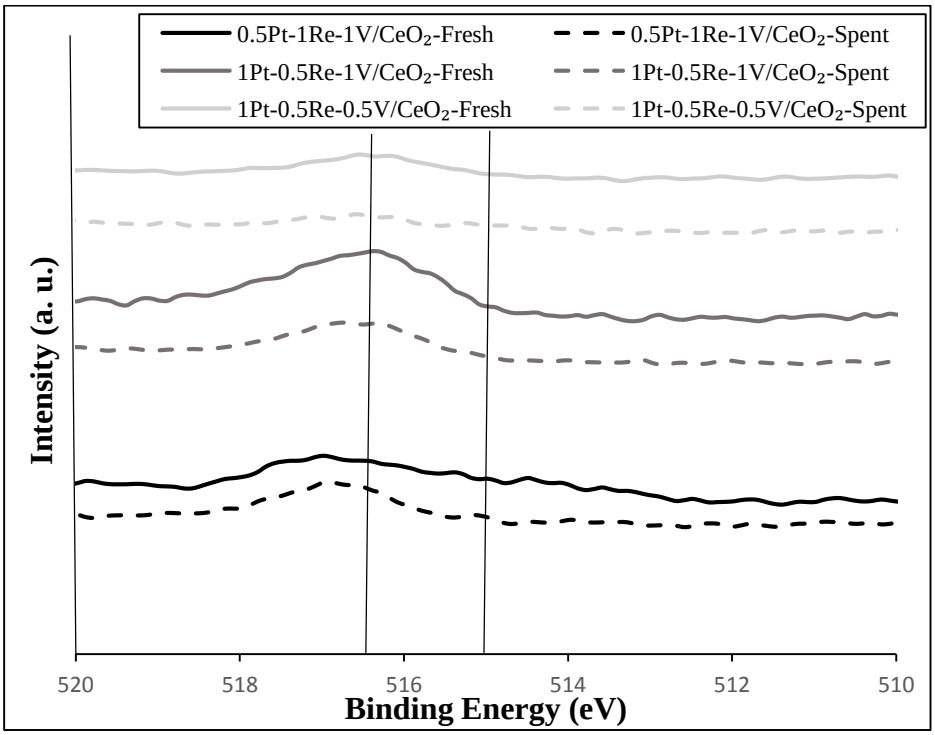

Figure 4.11. XP spectra showing the V 2p region of freshly reduced and spent catalyst samples (real feed #2, 350 °C).

Figure 4.12 displays the O 1s spectra of freshly reduced and spent catalysts. All freshly reduced catalysts showed peaks at 529 and 531 eV. These peaks correspond to oxygen in CeO_x lattice and chemisorbed water and hydroxyls, respectively (Çağlayan and Aksoylu, 2011). There is also a smaller peak at 533 eV which can be attributed to weakly adsorbed water only on the CeO_x in oxidized state. Comparably higher amounts of adsorbed water and hydroxyls are evident for the freshly reduced 0.5Pt-1Re-1V/CeO_2 sample. It was obvious that the peak at 529 eV was dramatically reduced in intensity after WGS reaction under high H_2O/CO feed conditions; whereas the peak at 531 eV increased rather slightly for all the catalyst samples. The decline at the intensity of the peak at 529 eV, which corresponds to oxygen in ceria lattice, indicates that CeO_2 takes crucial role in the reaction. The increase in the number of the surface hydroxyl groups and/or chemisorbed water might point out a reaction mechanism involving OH participation in the rate determining step when the feed is rich in water vapor. As a result of the WGS reaction under real feed #2 conditions, 527 eV peak corresponding to the lattice oxygen ions associated with a (−2) formal charge evolved at the low energy side

of the O 1s spectra for 1Pt-0.5Re-0.5V/CeO_2 (Caglayan and Aksoylu 2011). It should be noted that, this catalyst sample's surface Ce^{3+} concentration was increased under the same reaction conditions.

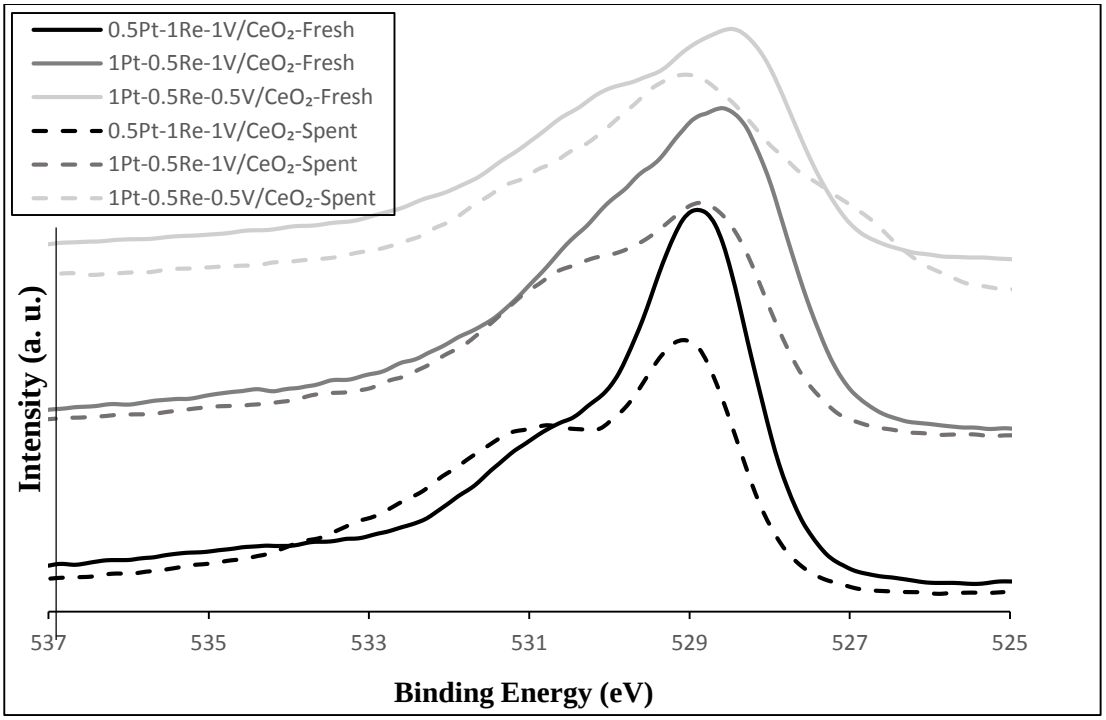

Figure 4.12. O 1s XP spectra of freshly reduced and spent catalyst samples (real feed #2, 350 °C).

In order to investigate the different surface oxygen species formed under different reaction conditions, Figure 4.13 is given presenting the O 1s spectra of the 1Pt-0.5Re-1V/CeO_2 catalyst before and after reaction under two different feed compositions with high and low H_2O/CO. This catalyst was specifically chosen for investigation because of its rather unexpected inferior performance when the H_2O/CO was increased. However, this performance could not be explained in view of the O 1s spectra as the spectra of both spent samples look similar with similar deconvolution results with a little shift in spectra to higher binding energy values.

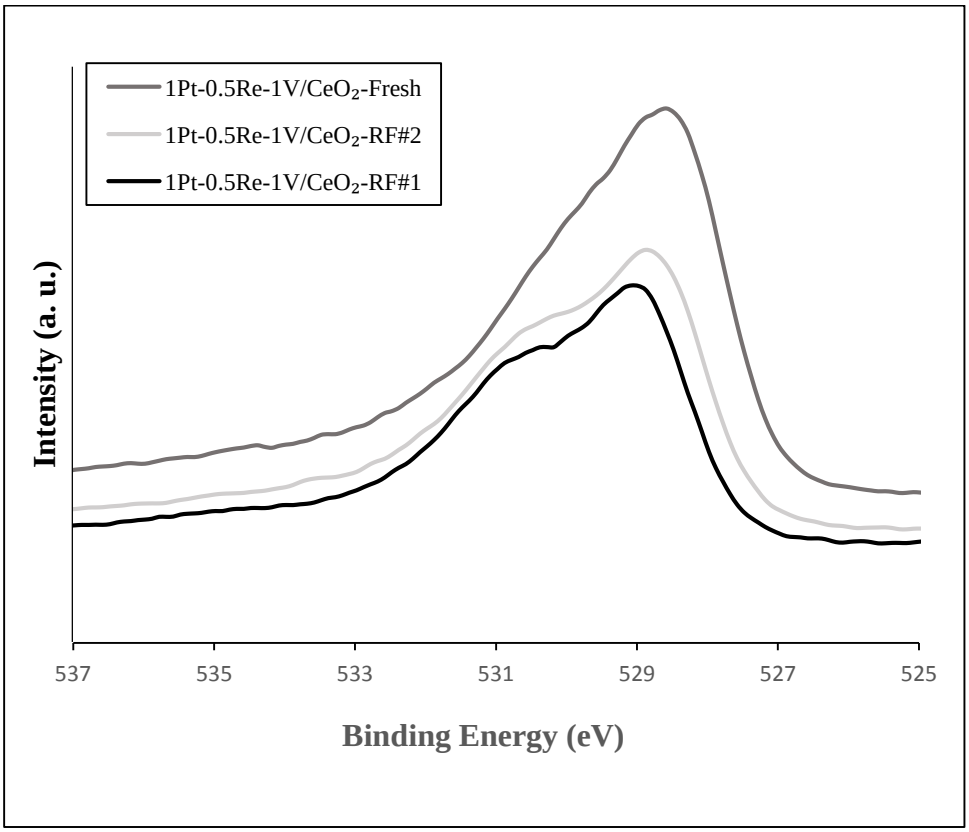

Figure 4.13. O 1s XP spectra of freshly reduced and spent 1Pt-0.5Re-1V/CeO_2 samples tested under two different real feed conditions at 350 °C.

The Pt 4f region of freshly reduced and spent catalysts at 350 °C with real feed #2 are shown in Figure 4.14. The peaks at 71.9 and 75.1 eV energy levels correspond to Pt^{2+} species; whereas the Pt $4f_{7/2}$ peak at 71.0 eV and the Pt $4f_{5/2}$ peak at 74.2 eV are assigned to Pt° (Pierre *et al*., 2007; Yu *et al*., 2010). And Pt^{2+} species are reported to be the active species for WGS reaction (Pierre *et al*., 2007- Roh *et al*., 2012). As seen from the graph, Pt^{2+} species dominantly formed on 1Pt-0.5Re-1V/CeO_2 and 0.5Pt-1Re-1V/CeO_2 samples. However 1Pt-0.5Re-0.5V/CeO_2 sample showed significant amount of Pt°, which is not active in WGS reaction and besides Pt° species were reported to cause annealing of ceria surface oxygen vacancies leading to surface area loss (Pierre *et al*., 2007). Since the mentioned catalyst has been proven to be active for the WGS reaction by the performance tests, the possibility of shift of the spectrum and therefore Pt^{2+} peaks to lower energy values should not be left out. Deconvolution analysis revealed there was no significant difference between the Pt^{2+} surface concentration of freshly reduced and

spent samples. The same results were also valid when the Pt 4f spectra of all the spent catalysts - catalyst tested under real feed #1 and #2 - were compared with the respective spectra of their freshly reduced formes (not shown).

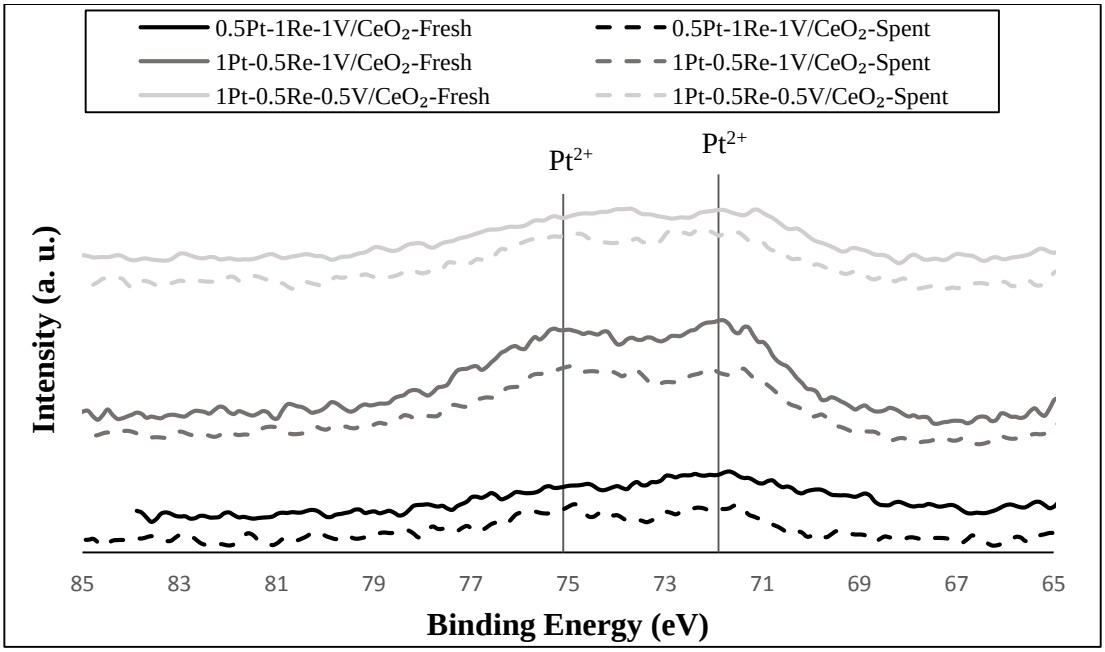

Figure 4.14. Pt 4f XP spectra of freshly reduced and spent catalyst samples (real feed #2, 350 °C).

Evaluation of the Re 4f spectra of the freshly reduced and spent catalyst samples have revealed that all Re surface species were in oxide form, which is in agreement with the literature; Re was reported to be in ReO_x form on CeO_2 supported catalysts (Azzam *et al.*, 2008).

4.2.2. Raman Spectroscopy

Raman spectroscopy is frequently used for analyzing the molecular structure of metal oxide species and is considered to be the most powerful technique for the characterization of metal oxides by observing vibrational, rotational, and other low frequency modes in the samples (Wu *et al.*, 2011).

Figure 4.15 illustrates the Raman spectra for freshly reduced Pt-Re-V/CeO_2 samples whereas Figure 4.16 is given to compare the Raman spectra of freshly reduced and spent catalysts. The spent catalysts in the performance tests were exposed to WGS reaction at 350 °C during 6 h TOS with real feed #1. The spectra are dominated by CeO_2 bands since ceria is the support material and it was reported to be a perfect Raman scatterer which overwhelms signal from surface vanadia species (Wu *et al.*, 2011). One sharp Raman main peak at around 460 cm^{-1} was observed for the bulk ceria in the spectra of all samples. Along with the main peak, the samples exhibited weak bands at around 265 cm^{-1} and 590 cm^{-1}, due to the presence of oxygen vacancies in the support (Hwang *et al*., 2011-Yu *et al*., 2011).

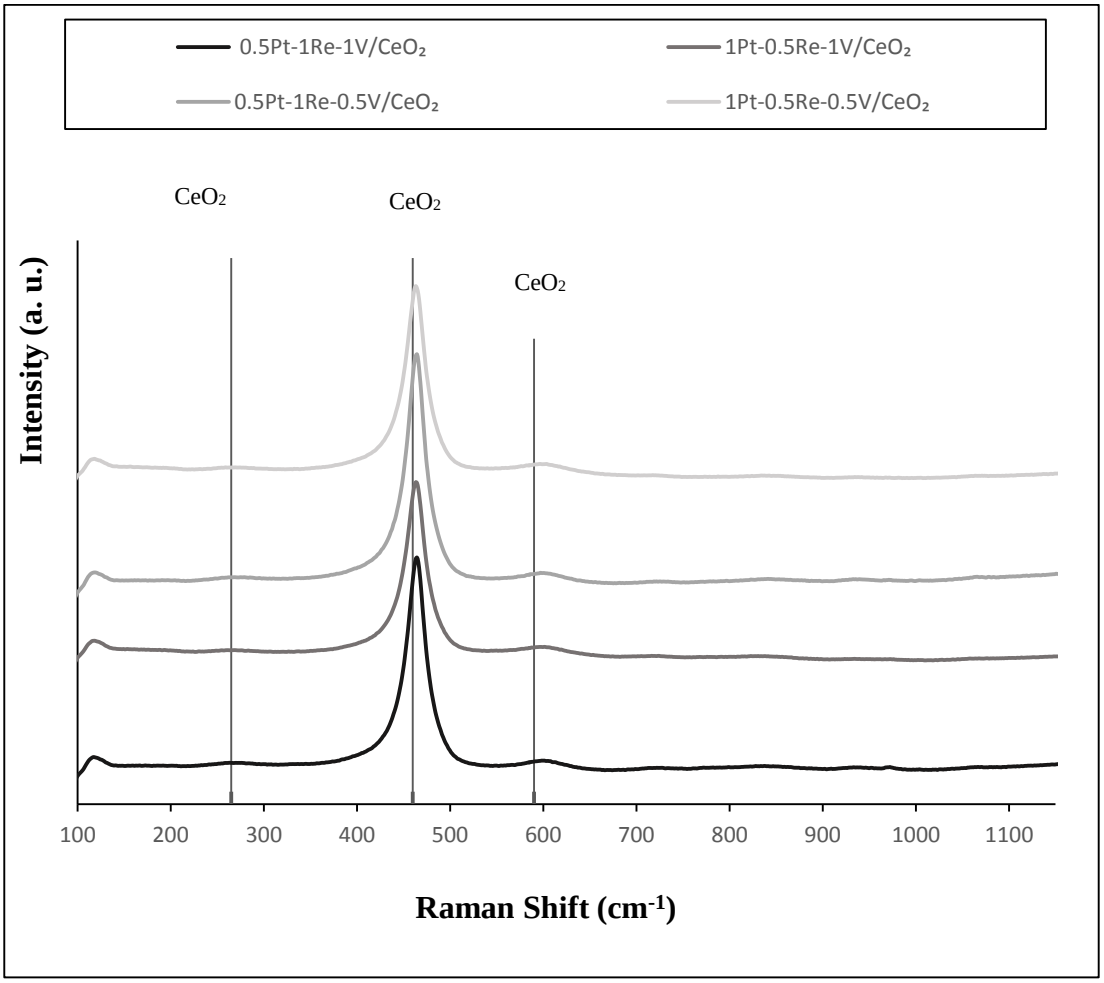

Figure 4.15. Raman spectra of freshly reduced catalyst samples (real feed #1, 350 °C).

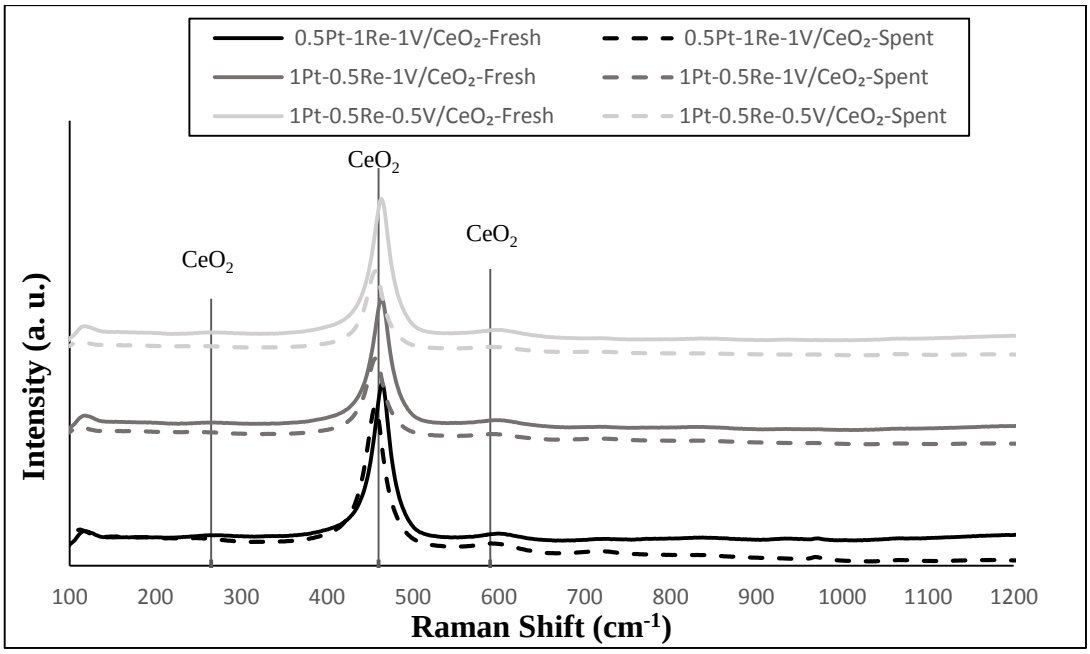

Figure 4.16. Raman spectra of the freshly reduced and spent (real feed #1, 350 °C) catalyst samples.

Through a comparative analysis of spectra obtained from fresh and spent samples in Figure 4.16, it was easy to spot a slight shift of bulk CeO_2 peak at ca. 460 cm^{-1}; the CeO_2 mode on spent catalysts shifted toward lower wavenumbers. It was previously reported by Rico-Frances *et al*. (2016) that the reason for this shift was the replacement of cerium atoms by other atoms, which determines the active role of CeO_2 in WGS reaction. In addition, the visible decrease in the intensity of the 460 cm^{-1} band for the spent 1Pt-0.5Re-1V/CeO_2 and 1Pt-0.5Re-0.5V/CeO_2 catalysts can be considered as an indicator of WGS activity since no visible difference in terms of intensity was observed on the CeO_2 mode at 460 cm^{-1} between freshly reduced and spent forms of 0.5Pt-1Re-1V/CeO_2, which has lower CO conversion levels.

Since the ceria main peak around 460 cm^{-1} is very dominant, the 550-1100 cm^{-1} interval in Figure 4.16 is given in the expanded form in Figure 4.17 in order to investigate the modes of the V species. The Raman spectra of all the freshly reduced and spent catalyst samples were observed to exibit Raman bands at around 720 and 830 cm^{-1} which were attributed to V-O-V stretching modes and to $CeVO_4$ species (Al-Ghamdi *et*

al., 2014, Martinez-Huerta *et al.*, 2008-Wu *et al.*, 2011). The 980 cm^{-1} band, appearing only in the spectra of relatively low performing 0.5Pt-1Re-1V/CeO_2 catalyst, was attributed to both stretching modes of V=O of V_2O_5 species and V-O-V in polyvanadate surface (Wu *et al.*, 2011-Al-Ghamdi *et al*., 2014). The increase in the intensity of this peak and 1060 cm^{-1} V=O peak (Wu *et al.*, 2011) after reaction is evident from Figure 4.17, however it should be noted that inactive V^{5+} presence was not observed in the XPS analysis.

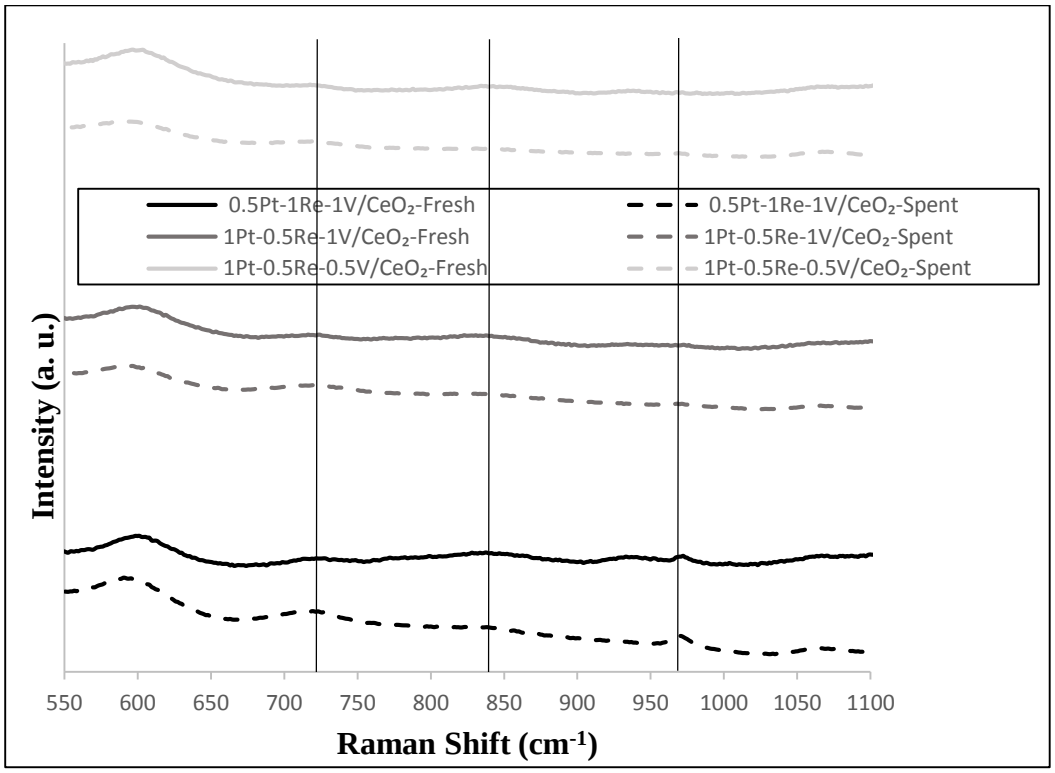

Figure 4.17. Raman spectra of the freshly reduced and spent (real feed #1, 350 °C).

It is important to note that no detectable bands for bulk V_2O_5 crystals (180, 235, 325, 345, 448, 520, 567 and 993 cm^{-1}) were observed in any of the samples (Al-Ghamdi *et al*., 2014). This result indicates that vanadium is highly dispersed at the surface without bulk V_2O_5 formation (Al-Ghamdi *et al*., 2014-Zhu *et al*., 2015).

In order to investigate the changes occurring on the surface under different reaction conditions, Figures 4.18 and 4.19 are given presenting the Raman spectra of the 1Pt-

0.5Re 1V/CeO_2 catalyst before and after reaction at 350 °C under two different feed compositions with high (16.2) and low (6.7) H_2O/CO ratio. A comparison between the Raman spectra of the two spent samples revealed that there is neither difference in the intensities nor the positions of the vanadium bands. However, the main bulk ceria band at ~460 cm^{-1} has lost intensity when the H_2O/CO ratio in the feed was increased indicating the further contribution of ceria in the reaction mechanism.

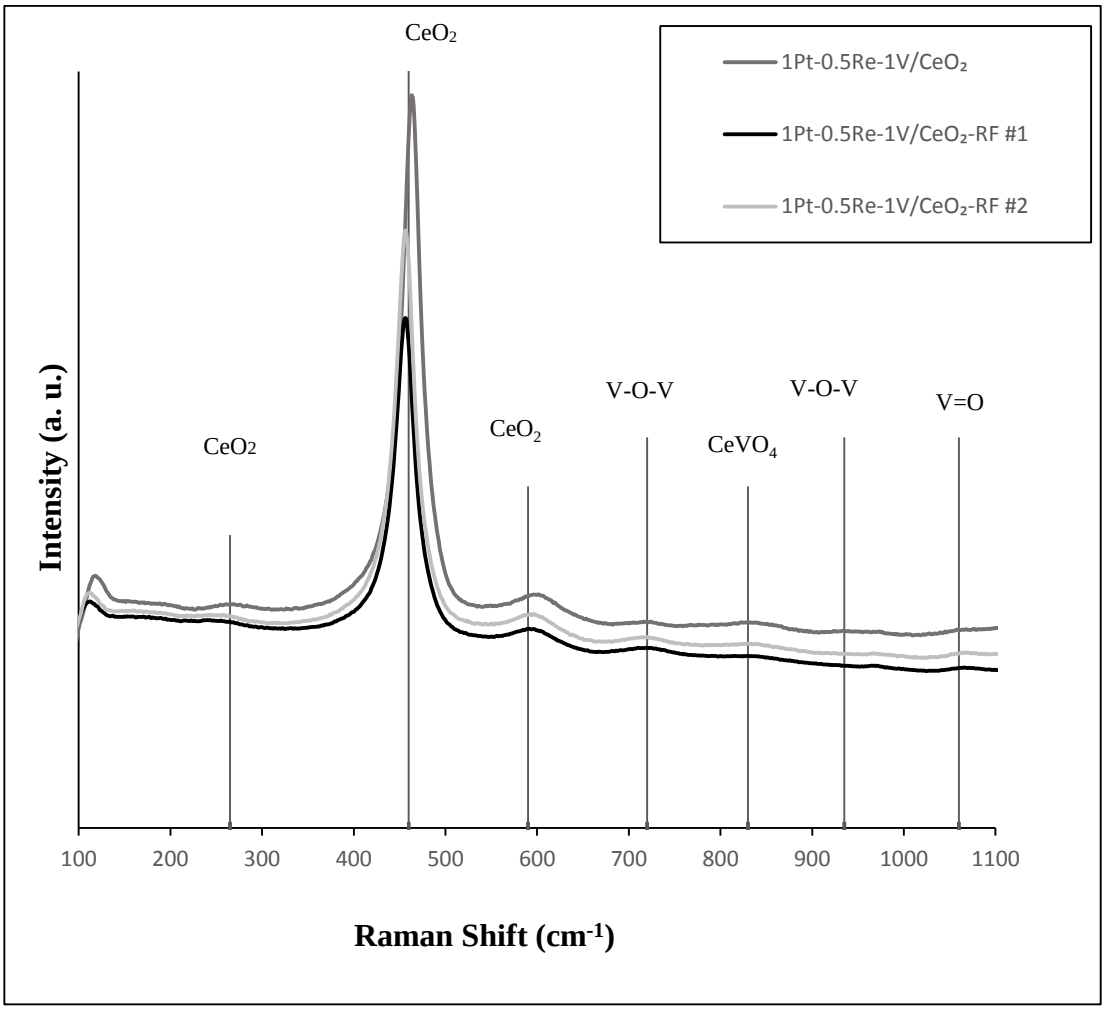

Figure 4.18. Raman spectra of the freshly reduced 1Pt-0.5Re-1V/CeO_2 catalyst sample and its spent forms tested under two different real feed conditions at 350 ˚C.

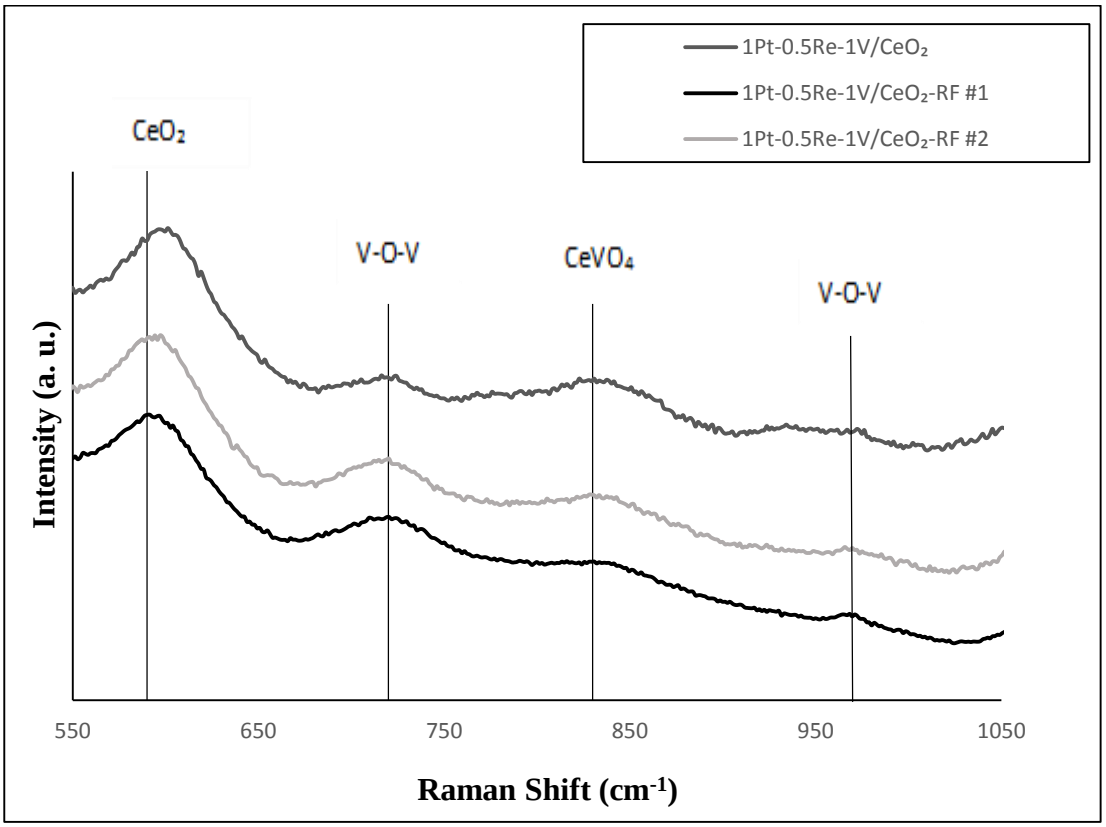

Figure 4.19. Expanded Raman spectra of the freshly reduced 1Pt-0.5Re-1V/CeO_2 catalyst sample and its spent forms tested under two different real feed conditions at 350 °C.

Figure 4.20 illustrates the Raman bands in the 1000-1800 cm^{-1} interval of the Raman spectra of the spent catalyst samples after WGS reaction of 6 h TOS at 350 °C under the flow of real feeds. Raman spectroscopy can be used to analyze the structure of carbon, which was deposited on the spent catalysts. Disordered structural mode of crystalline carbon species and graphitic carbon with high degree of symmetry are represented by the D and G bands, which are located at 1360 and 1600 cm^{-1} (Paksoy *et al.*, 2015, Wragg *et al.*, 2013, De Souse *et al*., 2012). Although the intensities of the D and G bands are very low indicating nearly no coke formation, relatively higher intensity of D and G bands on the Raman spectrum of spent 0.5Pt-1Re-1V/CeO_2 sample for which CO conversion levels were low, were observed.

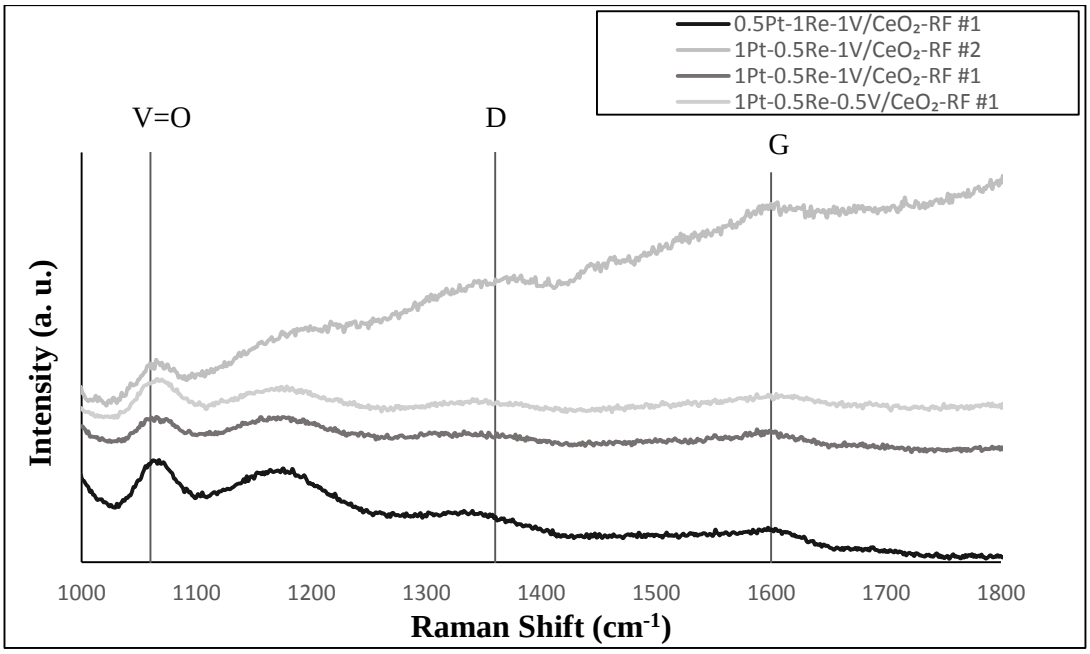

Figure 4.20. Raman spectra (1000-1800 cm^{-1}) of spent catalyst samples tested under two different real feed conditions at 350 °C.

No bands corresponding to low frequency modes of Re and Pt metal oxides in any of the Raman spectra of the freshly reduced and spent catalyst samples which may point out the incorporation of these atoms into the CeO_2 lattice (Rico-Frances *et al*., 2016).

5. CONCLUSION

5.1. Conclusions

The purpose of this experimental study is to design and develop Pt-based, CeO_2 supported trimetallic Pt-Re-V/CeO_2 catalysts(s) having high WGS activity, selectivity and stability with suppressed methanation under realistic feed *(i.e. feeds simulating typical reformer outlet)* flow in HTS-LTS transition temperature region, allowing the use of a single WGS reactor in fuel processors. Pt- Re- and V- loading levels were 0.5 and 1 wt.% in the trimetallic catalysts. The major conclusions of this study can be summarized as follows:

The results revealed that 1Pt-0.5Re-1V/CeO_2 and 1Pt-0.5Re-0.5V/CeO_2 have great potentials to be used in a fuel processor as a WGS catalyst owing to their high activity, stability and selectivity. Another important point is that those catalysts can make the use of a single stage WGS unit in an FP possible instead of conventional two stage (HTS and LTS) WGS unit.

The performance results clearly revealed that the catalysts reached their highest performance at 350 °C, most probably due to suppression of CO conversion due to lower themodynamic equilibrium at 400 °C.

Comparative analysis of the results indicated that more stable activities were obtained for the whole temperature range, 300-400 °C, when real feed #2, which has higher H_2O/CO ratio, was used. The highest net hydrogen production rates were observed over 1Pt-0.5Re-1V and 1Pt-0.5Re-0.5V samples for H_2O/CO poor and rich feed streams, respectively. Changing feed composition from real feed #1 to real feed #2, resulted in comparable activities on 1Pt-0.5Re-0.5V/CeO_2. However, for the other three catalysts, increasing H_2O/CO ratio of the feed led to a better performance at 300 °C, whereas to a decrease in CO conversion at 400 °C. Furthermore, this change in the feed stream resulted in a decrease in the net H_2 production values for all catalysts.

0.5% Pt loaded samples had inferior performance under the flow of both feeds. The findings confirm crucial role of Pt-Re interaction in H_2O activation, and hints that when Re:V ratio is low, the contribution of Re to performance in water rich conditions is suppressed.

Ce^{3+} content is reported to be slightly higher in the case of the catalysts with higher WGS activity. As a result of the electron transfer during reaction, the amount of Ce^{3+} is expected to decrease for the catalyst samples upon reaction. Accordingly, the % decrease in the Ce^{3+} content for the better performing 1Pt-0.5Re-1V/CeO_2. The increase in the Ce^{3+} content for 1Pt-0.5Re-0.5V/CeO_2 catalyst sample after reaction was considered as an experimental error. The increase in the number of the surface hydroxyl groups and/or chemisorbed water might point out a reaction mechanism involving OH participation in the rate determining step when the feed is rich in water vapor.

XPS and Raman spectroscopy results showed that $CeVO_4$ species and VO_2 compound, which has been reported to have promotion effect in the WGS activity, were present on the catalyst. It is important to note that no detectable bands for bulk V_2O_5 crystals were observed in any of the samples. This result indicates that vanadium is highly dispersed at the surface without bulk V_2O_5 formation. Moreover, no coke formation was observed on any spent samples.

5.2. Recommendations

Following ideas are suggested for future studies of Pt-Re-V/CeO_2 as a selective WGS catalyst:

- FTIR-DRIFTS study representation for the investigation of reaction mechanisms.
- Performance tests on 0.5Pt-0.5Re-0.5V/CeO_2 catalyst composition.
- Performing kinetic studies for obtaining a power-law type WGS rate expression.

- Performance tests on serial OSR-WGS-(PROX) reactor system to see the **real** performance of 1Pt-0.5Re-1V/CeO_2 and 1Pt-0.5Re-0.5V/CeO_2 WGS catalysts.

- Testing robustness of WGS catalysts during transient fuel processor operations involving exposure of catalyst to air and liquid water.

REFERENCES

Al-Ghamdi, S. A. and H. I. de Lasa, 2014, "Propylene Production via Propane Oxidative Dehydrogenation over Vo_x/γ-Al_2O_3 Catalyst", *Fuel*, Vol. 128, pp. 120-140.

Andreeva, D., V. Idakiev, T. Tabakova, L. Ilieva, P. Falaras, A. Bourlinos and A. Travlos, 2002, "Low-Temperature Water-Gas Shift Reaction over Au/CeO_2 Catalysts", *Catalysis Today*, Vol. 72, pp. 51-57.

Aranifard, S., 2013, *Theoretical Investigation of the Water Gas Shift Reaction at the Three Phase Boundary of Ceria Supported Platinum Metal Clusters*, Ph.D. Dissertation, University of South Carolina.

Avcı, A. K., Z. I. Önsan and D. L. Trimm, 2001, "On-board Fuel Conversion for Hydrogen Fuel Cells: Comparison of Different Fuels by Computer Simulations", *Applied Catalysis A: General*, Vol. 216, pp. 243-256.

Azzam, K. G., I. V. Babich and S. L. Leffers, 2007a, "Bifunctional Catalysts for Single-Stage Water-Gas Shift Reaction in Fuel Cell Applications. Part 1. Effect of the Support on the Reaction Sequence", *Journal of Catalysis,* Vol. 251, pp. 153-162.

Azzam, K. G., I. V. Babich and S. L. Leffers, 2007b, "A Bifunctional Catalyst for the Single-Stage Water-Gas Shift Reaction in Fuel Cell Applications. Part 2. Roles of the Support and Promoter on Catalyst Activity and Stability", *Journal of Catalysis,* Vol. 251, pp. 163-171.

Azzam, K. G., I. V. Babich, K. Seshan and L. Lefferts, 2008, "Role of Re in $Pt\text{-}Re/TiO_2$ Catalyst for Water Gas Shift Reaction: A Mechanistic and Kinetic Study", *Applied Catalysis B: Environmental*, Vol. 80, pp. 129-140.

Azzam, K. G., I. V. Babich, K. Seshan, B. L. Mojet and L. Lefferts, 2013, "Stable and Efficient Pt-Re/TiO_2 Catalysts for Water-Gas-Shift: On the Effect of Rhenium", *ChemCatChem*, Vol. 5, pp. 557-564.

Ballarini, N., A. Battisti, F. Cavani, A. Cericola, C. Lucarelli, S. Racioppi and P. Arpentinier, 2006, "The Oxygen-Assisted Transformation of Propane to CO_x/H_2 through Combined Oxidation and WGS Reactions Catalyzed by Vanadium-Oxide Based Catalysts", *Catalysis Today*, Vol. 116, pp. 313-323.

Bautista F.M., Campelo J.M., Luna D., Luque J., Marinas J.M. 2006. Influence of the Acid-Base/Redox Properties of TiO*x*-Sepiolite Supported Vanadium Oxide Catalysts in the Gas-Phase Selective Oxidation of Toluene, *Catalysis Today*, Vol. 112, pp. 28-32.

Boyesen K.L., Kristiansen T., Mathisen K. 2015, "Dynamic Redox Properties of Vanadium and Copper in Microporous Supports During the Selective Oxidation of Propene", *Catalysis Today*, Vol. 254, pp. 21-28.

Barreto, L., A. Makihira and K. Riahi, 2003, "The Hydrogen Economy in the 21st Century: A Sustainable Development Scenario", *International Journal of Hydrogen Energy*, Vol. 28, pp. 267-284.

Boaro, M., M. Vicario, J. Llorca, C. Leitenburg, G. Dolcetti and A. Trovarelli, 2009, "A Comparative Study of Water Gas Shift Reaction over Gold and Platinum Supported on ZrO_2 and CeO_2-ZrO_2", *Applied Catalysis B: Enviromental*, Vol. 88, pp. 272-282.

Çağlayan, B. S. And A. E. Aksoylu, 2009, "Water-Gas Shift Reaction over Bimetallic Pt-Ni/Al_2O_3 Catalysts", *Turkish Journal of Chemistry*, Vol. 33, pp. 249-256.

Çağlayan, B. S. and A. E. Aksoylu, 2011, "Water-Gas Shift Activity of Ceria Supported Au–Re Catalysts", *Catalysis Communications*, Vol. 12, pp. 1206-1211.

Çağlayan, B. S., A. K. Avcı, Z. I. Önsan, and A. E. Aksoylu, 2005, "Production of Hydrogen over Bimetallic Pt–Ni/δ-Al_2O_3: I. Indirect Partial Oxidation of Propane", *Applied Catalysis A: General*, Vol. 280, pp. 181-188.

Campbell, C. T. and C. H. F. Peden, 2005, "Oxygen Vacancies and Catalysis on Ceria Surfaces", *Science*, Vol. 309, pp. 713-714.

Castaño, M. G., T. R. Reine, S. Ivanova, M. A. Centeno and J. A. Odriozola, 2014, "Pt vs. Au in Water–Gas Shift Reaction", *Journal of Catalysis*, Vol. 314, pp. 1-9.

Chen, W. H., M. R. Lin, J. J. Lu, Y. Chao and T. S. Leu, 2010, "Thermodynamic Analysis of Hydrogen Production from Methane via Autothermal Reforming and Partial Oxidation Followed by Water Gas Shift Reaction" *International Journal of Hydrogen Energy*, Vol. 32, pp. 11787-797.

Choung, S. Y., M. Ferrandon, T. Krause, 2004, "Pt-Re Bimetallic Supported on CeO_2-ZrO_2 Mixed Oxides as Water-Gas Shift Catalysts", *Catalysis Today*, Vol. 99, pp. 257-262.

De Sousa, F.F., H.S.A. De Sousa, A.C. Oliveira, M.C.C. Junioe, A.P. Ayala, E.B. Barros, B.C Viana, J.M. Filho, A.A. Oliveira, 2012, "Nanostructured Ni-Containing Spinel Oxides for the Dry Deforming of Methane: Effect of the Presence of Cobalt and Nickel on the Deactivation Behaviour of Catalysts", *Hydrogen Energy*, Vol. 37, pp. 3201-3212.

Demeter, M., M. Neumann and W. Reichelt, 2000, "Mixed-Valence Vanadium Oxides Studied By XPS", *Surface Science*, Vol. 454-456, pp. 41-44.

Duarte de Farias, A. M., P. Bargiela, M. d. G. C. Rocha and M. A. Fraga, 2008, "Vanadium-Promoted Pt/CeO_2 Catalyst for Water-Gas Shift Reaction", *Journal of Catalysis*, Vol. 260, pp. 93-102.

Dudfield, C. D., R. Chen, P.L. Adcock, 2001, "A Carbon Monoxide PROX Reactor for PEM Fuel Cell Automotive Application" *International Journal of Hydrogen Energy,* Vol. 26, pp. 763-775.

El-Moemen, A. A., G. Kučerová and R.J. Behm, 2010, Influence of H_2, CO_2 and H_2O on the Activity and Deactivation Behavior of Au/CeO2 Catalysts in the Water Gas Shift Reaction at 300 °C", *Applied Catalysis B: Environmental,* Vol. 95, pp. 57–70.

Esch, F., S. Fabris, L. Zhou, T. Montini, C. Africh, P. Fornasiero, G. Comelli and R. Rosei, 2005, "Electron Localization Determines Defect Formation on Ceria Substrates", *Science,* Vol. 309, pp. 752-755.

Fu, Q., A. Weber and M. Flytzani-Stephanopoulos, 2001, "Nanostructured Au–CeO2 Catalysts for Low-Temperature Water–Gas Shift", *Catalysis Letters,* Vol. 77, pp. 87-95.

Fu, Q., H. Saltsburg and M. Flytzani-Stephanopoulos, 2003, "Active Nonmetallic Au and Pt Species on Ceria-Based Water-Gas Shift Catalysts", *Science,* Vol. 301, pp. 935-938.

Galvita, V. and K. Sundmacher, 2007 "Cyclic Water Gas Shift Reactor (CWGS) for Carbon Monoxide Removal From Hydrogen Feed Gas for PEM Fuel Cells", *Chemical Engineering Journal,* Vol. 134, pp.168-174.

Galvita, V., K. Sundmacher, 2007, "Cyclic Water Gas Shift Reactor (CWGS) for Carbon Monoxide Removal From Hydrogen Feed Gas for PEM Fuel Cells" *Chemical Engineering Journal,* Vol. 134, pp. 168-174.

Germani, G, P. Alphonse, M. Courty, Y. Schurman, C. Mirodatos, 2005, "Platinum/Ceria/Alumina Catalysts on Microstructures for Carbon Monoxide Conversion", *Catalysis Today,* Vol. 110, pp. 114-120.

Gewade, P., B. Mirkelamoglu, B. Tan, U. S. Ozkan, "Cr-free Fe-based Water Gas Shift Catalysts Prepared Through Propylene Oxide-Assisted Sol-Gel Technique", *Journal of Molecular Catalysis A: Chemical*, Vol. 321, pp. 61-70.

Gökaliler, F., B. A. Göçmen and A. E. Aksoylu, 2008, "The Effect of Ni:Pt Ratio on Oxidative Steam Reforming Performance of Pt-Ni/Al_2O_3 Catalyst", *International Journal of Hydrogen Energy*, Vol. 33, pp. 4358-4366.

Guo, P., L. Chen, Q. Yang, M. Qiao, H. Li, H. Li, H. Xu and K. Fan, 2009a, Cu/ZnO/Al_2O_3 Water-Gas Shift Catalysts for Practical Fuel Cell Applications: The Performance in Shut-Down/Start-Up Operation", *International Journal of Hydrogen Energy*, Vol. 34, pp. 2361-2368.

Haber J., A. Kozlowska, R. Kozlowski, 1986, "The Structure and Redox Properties of Vanadium Oxide Surface Compounds", *Catal*, Vol. 102, pp. 52-63.

Hwang, K., J. Park and S. Ihm, 2011, "Si-Modified Pt/CeO_2 Catalyst for a Single-Stage Water-Gas Shift Reaction", *International Journal of Hydrogen Energy*, Vol. 36, pp. 9685-9693.

Iida, H. and A. Igarashi, 2006, "Structure Characterization of Pt-Re/TiO_2 (Rutile) and Pt-Re/ZrO_2 Catalysts for Water Gas Shift Reaction at Low-Temperature", *Applied Catalysis A: General*, Vol. 303, pp. 192-198.

Junior, I. L., J. M. Millet, M. Aouine and M. C. Rangel, 2005, "The Role of Vanadium on the Properties of Iron Based Catalysts for the Water Gas Shift Reaction", *Applied Catalysis A: General*, Vol. 283, pp. 91-98.

Kalamaras, C. M., I. D. Gonzalez, R. M. Navarro, J. L. G. Fierro and A. M. Efstathiou, 2011, "Effects of Reaction Temperature and Support Composition on the

Mechanism of Water-Gas Shift Reaction over Supported-P Catalysts", *The Journal of Physical Chemistry*, Vol. 115, pp. 11595-11610.

Kalamaras, C. M., S. Americanou and A. M. Efstathiou, 2011, "Redox vs Associative Formate with -OH Group Regeneration WGS Reaction Mechanism on Pt/CeO_2: Effect of Platinum Particle Size", *Journal of Catalysis*, Vol. 279, pp. 287-300.

Kam, R., J. Scott, R. Amal and C. Selomulya, 2010, "Pyrophoricity and Stability of Copper and Platinum Based Water-Gas Shift Catalysts during Oxidative Shut-Down/Start-Up Operation", *Chemical Engineering Science*, Vol. 65, pp. 6461-6470.

Kugai, J., J. T. Miller, N. Guo and C. Song, 2011a, "Oxygen-Enhanced Water Gas Shift on Ceria-Supported Pd-Cu and Pt-Cu Bimetallic Catalysts", *Journal of Catalysis*, Vol. 277(1), pp. 46–53.

Lee, I. C. and D. Chu, 2003, *Literature Review of Fuel Processing*, Army Research Laboratory.

Lee, D., M. S. Lee, J. Y. Lee, S. Kim, H. Eom, D. J. Moon and K. Lee, 2013, "The Review of Cr-free Fe-based Catalysts for High-Temperature Water-Gas Shift Reactions", *Catalysis Today*, Vol. 210, pp. 2-9.

Lenite, B. A., C. Galletti and S. Specchia, 2011, "Studies on Au Catalysts for Water Gas Shift Reaction", *International Journal of Hydrogen Energy*, Vol. 36, pp. 7750-7758.

Leppelt, R., B. Schumacher, V. Plzak, M. Kinne and R. J. Behm, 2006, "Kinetics and Mechanism of the Low-Temperature Water-Gas Shift Reaction on Au/CeO_2 Catalysts in an Idealized Reaction Atmosphere", *Journal of Catalysis*, Vol. 244, pp. 137-152.

LeValley, T. L., A. R. Richard and M. Fan, 2014, "The Progress in Water Gas Shift and Steam Reforming Hydrogen Production Technologies–A Review", *International Journal of Hydrogen Energy*, Vol. 39, pp. 16983-17000.

Liu X., W. Ruettinger, X. Xu, R. Farrauto, 2005, "Deactivation of Pt/CeO_2 Water-Gas Shift Catalysts due to Shutdown/Startup Modes for Fuel Cell Applications", *Applied Catalysis B: Enviromental,* Vol. 56, pp. 69-75.

M. Shelef, G.W. Graham and R.W. McCabe, 2002, "Catalysis by Ceria and Related Materials" *ed. A. Trovarelli Imperial College Press, London*, ch. 10.

Maroño, M., E. Ruiz, J. M. Sànches, C. Martos, J. Dufour and A. Ruiz, "Performance of Fe-Cr Based WGS Catalysts Prepared by Co-Precipitation and Oxi-Precipitation Methods" , *International Journal of Hydrogen Energy,* Vol. 34, pp. 8921-8928.

Martinez-Huerta, M. V., G. Deo, J. L. G. Fiberro and M. A. Bañares, 2008, "Operando Raman-GC Study on the Structure-Activity Relationships in V^{5+}/CeO_2 for Catalyst Ethane Oxidative Dehydrogenation: The Formation of $CeVO_4$", *The Journal of Physical Chemistry C,* Vol. 112, pp. 11441-11447.

Martinez-Huerta, M. V., X. Gao, H. Tian, I. E. Wachs, J. L. G. Fierro and M. A. Bañares, 2006, "Oxidative Dehydrogenation of Ethane to Ethylene Over Alumina-Supported Vanadium Oxide Catalysts: Relationship Between Molecular Structures and Chemical Reactivity", *Catalysis Today,* Vol. 118, pp. 279-287.

Moe, J.M., 1962, "Design of Water-Gas Shift Reactors", *Chemical Engineering Progress*, Vol. 58, pp. 33-36.

Natesakhawat, S., X. Wang, L. Zhang and U.S. Ozkan, 2006, "Development of Chromium-free Iron-Based Catalysts for High-Temperature Water-Gas Shift Reaction", *Journal of Molecular Catalysis A: Chemical,* Vol. 260, pp. 82-94.

Navarro, R.M., M.A. Pena and J.L.G. Fierro, 2007, "Hydrogen Production Reactions from Carbon Feedstocks: Fossil Fuels and Biomasses", *Chemical Reviews*, Vol. 107, pp. 3952-3991.

Nishimura, S., T. Shishido, K. Ebitani, K. Teramura and T. Tanaka, 2010, "Novel Catalytic Behavior of Cu/Al_2O_3 Catalyst Against Daily Start-Up and Shut-Down (DSS)-like Operation in the Water Gas Shift Reaction", *Applied Catalyst A: General*, Vol. 387, pp. 185-194.

Paksoy, A. İ., B. S. Çağlayan and A. E. Aksoylu, 2015, "A Sudy on Characterization and Methane Dry Reforming Performance of $Co\text{-}Ce/ZrO_2$ Catalyst", *Applied Catalysis B: Environmental*, Vol. 168-169, pp. 164-174.

Panagiotopoulou, P. and D.I. Kondarides, 2006, "Effect of the Nature of the Support on the Catalytic Performance of Noble Metal Catalysts for the Water–Gas Shift Reaction", *Catalysis Today*, Vol. 112, pp. 49-52.

Panagiotopoulou, P., J. Papavasiliou, G. Avgouropoulos, T. Ionnides and D. I. Kondarides, 2007, "Water-Gas Shift Activity of Doped Pt/CeO_2 Catalysts", *Chemical Engineering Journal*, Vol. 134, pp. 16-22.

Pierre, D., W. Deng and M. F. Stephanopoulos, 2007, "The Importance of Strongly Bound $Pt\text{-}CeO_x$ Species for the Water-gas Shift Reaction: Catalyst Activity and Stability Evaluation", *Topics in Catalysis*, Vol. 46, pp. 363-373.

Popa, T., G. Xu, T. F. Barton and M. D. Argyle, "High Temperature Water Gas Shift Catalysts with Alumina", *Applied Catalysis A: General*, Vol. 379, pp. 15-23.

Rakesh Radhakrishnan, R., R. R. Willigan, Z. Dardas and T. H. Vanderspurt, 2006a, "Water Gas Shift Activity of Noble Metals Supported on Ceria-Zirconia Oxides", *AIChE Journal*, Vol. 52, pp. 1888-1894.

Ratnasamy, C., J. P. Wagner and S. Chemie, 2009, "Water Gas Shift Catalysis", *Catalysis Reviews: Science and Engineering*, Vol. 51, No. 3, pp. 325-440.

Rico- Francés, S., E. O. Jardim, T. A. Wezendonk, F. Kapteijn, J. Gascon, A. S. Escribano and E. V. Ramos-Fernandez, 2016, "Highly Dispersed $Pt^{\delta+}$ on $Ti_xCe_{(1-x)}O_2$ as an Active Phase in Preferential Oxidation of CO", *Applied Catalyst B: Environmental*, Vol. 180, pp. 169-178.

Roh, H. S., H. S. Potdar, D. W. Jeong, K. S. Kim, J. O. Shim, W. J. Jang, K. Y. Koo, W. L. Yoon, 2012, "Synthesis of Highly Active Nano-sized (1 wt.% Pt/CeO_2) Catalyst for Water Gas Shift Reaction in Medium Temperature Application", *Catalysis Today*, Vol. 185, pp. 113-118.

Ruettinger W., O. Ilinich, S. Lee (Ed), "Encyclopedia of Chemical Processing", *Taylor & Francis*, Vol: 1, pp. 3205.

Sato, Y., K. Terada, S. Hasegawa, T. Miyao and S. Naito, 2005, "Mechanistic Study of Water-Gas-Shift Reaction over TiO_2 Supported Pt-Re and Pd-Re Catalysts", *Applied Catalysis*, Vol. 296, pp. 80-89.

Sato, Y., K. Terada, Y. Soma, T. Miyao, S. Naito, 2006, "Marked Addition Effect of Re Upon the Water Gas Shift Reaction Over TiO_2 Supported Pt, Pd and Ir catalysts", *Catalysis Communication*, Vol. 7, pp. 91-95.

Sharma, S. and S. K. Ghoshal, 2015, "Hydrogen for Future Transportation Fuel: From Production to Applications", *Renewable and Sustainable Energy Reviews*, Vol. 43, pp. 1151-1158.

Shekhawat, D., J. J. Spivey, D. A. Berry, 2011, "Fuel Cells: Technologies for Fuel Processing", *Elsevier*.

Silversmit, G., D. Depla, H. Poelman, G. B. Marin and R. D. Gryse, 2004, "Determination of the V2p XPS Binging Energies for Different Vanadium Oxidation States (V^{5+} to $V^{\circ+}$)", *Journal of Electron Spectroscopy and Related Phenomena*, Vol. 135, pp. 167-175.

Suchorski, Y., L. R. Struckmann, F. Klose, Y. Ye, M. Alandjiyska, K. Sundmacher and H. Weiss, 2005, "Evolution of Oxidation States in Vanadium-based Catalysts under Conventional XPS Conditions", *Applied Surface Science*, Vol. 249, pp. 231-237.

Tabakova, T., F. Boccuzzi, M. Manzoli and D. Andreeva, 2003, "FTIR Study of Low-Temperature Water-Gas Shift Reaction on Gold/Ceria Catalyst", *Applied Catalyst A: General*, Vol. 252, pp. 385-397.

Tanksale, A., J.N. Beltramini, and G.M. Lu, 2010, "A Review of Catalytic Hydrogen Production Processes from Biomass", *Renewable and Sustainable Energy Reviews*, Vol. 14, pp. 166–182.

Thanh, D. N., A. M. Duarte de Farias, M. A. Fraga, 2008, "Characterization and Activity of Vanadia-Promoted Pt/ZrO_2 for the Water-Gas Shift Reaction", Catalysis Today, Vol. 138, pp. 235-238.

Trimm, D. L., 2005, "Minimisation of Carbon Monoxide in a Hydrogen Stream for Fuel Cell Application", *Applied Catalysis A: General*, Vol. 296, pp. 1-11.

Wragg, D.S., Gronvold, A., Norby, P., Fjellvag. H. 2013. Combined XRD and Raman studies of coke types found in SAPO-34 after methanol and propene conversion, Microporous Mesoporous Mater. 173, 166–174.

Wu Z., A. J. Rondinone, I. N. Ivanov and S. H. Overbury, 2011, "Structure of Vanadium Oxide Supported on Ceria by Multiwavelength Raman Spectroscopy", *The Journal of Physical Chemistry C*, Vol. 115, pp. 25368-25378.

Yu, J., F. J. Tian and C. Z. Li, 2006, "Char-Supported Nano Iron Catalyst for Water-Gas Shift Reaction: Hydrogen Production from Coal/Biomass Gasification, "*Process Safety and Enviromental Protection,* Vol. 84, pp. 125-130.

Yu, Q., W. Chen, Y. Li, M. Jin and Z. Suo, 2010, "The Action of Pt in Bimetallic Au-Pt/CeO_2 Catalyst for Water-Gas Shift Reaction", *Catalysis Today*, Vol. 158, pp. 324-328.

Yu, Q., X. Wu, C. Tang, L. Qi, B. Liu, F. Gao, K. Sun, L. Dong and Y. Chen, 2011, "Textural, Structural, and Morphological Characterizations and Catalytic Activity of Nanosized CeO_2-MOx (M=Mg^{2+}, Al^{3+}, Si^{4+}) Mixed Oxides for CO Oxidation", *Journal of Colloid and Interface Science*, Vol. 354, pp. 341-352.

Zhu, H., S. Ould-Chikh, H. Dong, I. Llorens, Y. Saih, D. H. Anjum, J. L. Hazemann and J. M. Basset, 2015, "VOx/SiO_2 Catalyst Prepared by Grafting $VOCl_3$ on Silica for Oxidative Dehydrogenation of Propane", *ChemCatChem*, Vol. 7, pp. 3332-3339.

Zhu, X., M. Shen, L. L. Lobban and R. G. Mallinson, 2011, "Structural Effects of Na Promotion for High Water Gas Shift Activity on Pt-Na/TiO_2", *Journal of Catalysis*, Vol. 278, pp. 123-132.

APPENDIX A: TIME-ON-STREAM ACTIVITY DATA

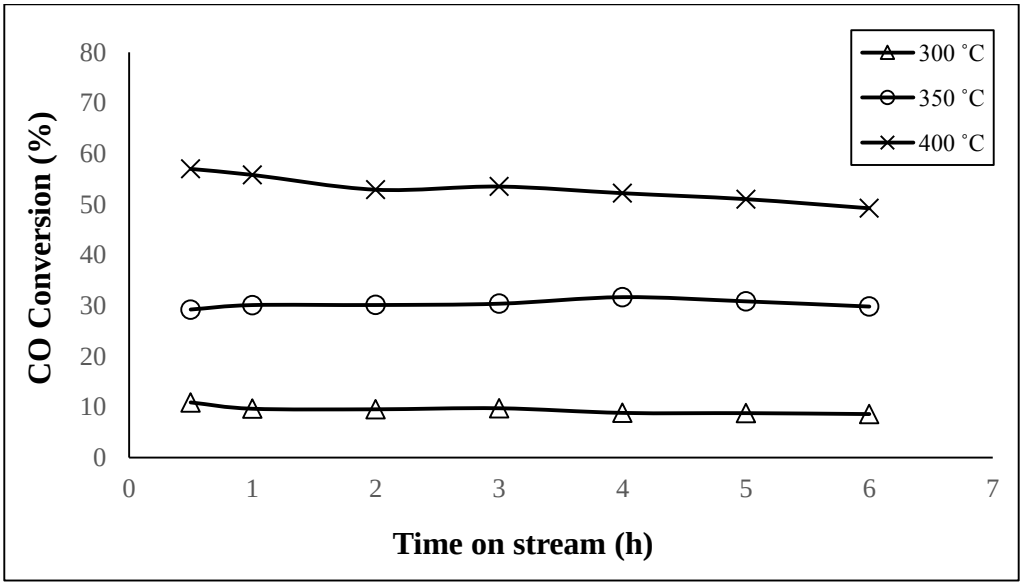

Figure A.1. Temperature dependence of time-on-stream activity data of 0.5Pt-1Re-1V/CeO_2 for real feed #1.

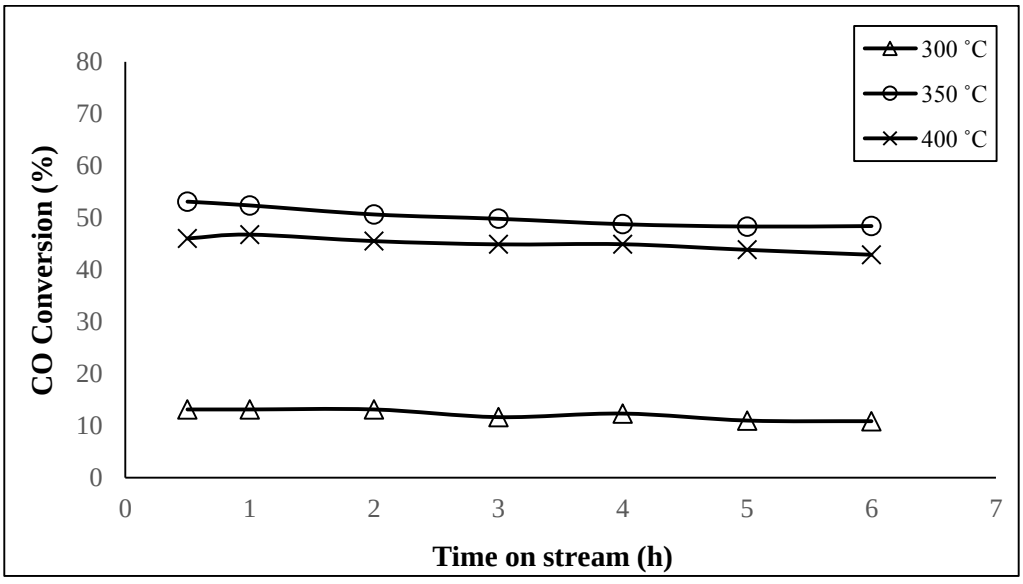

Figure A.2. Temperature dependence of time-on-stream activity data of 0.5Pt-1Re-1V/CeO_2 for real feed #2.

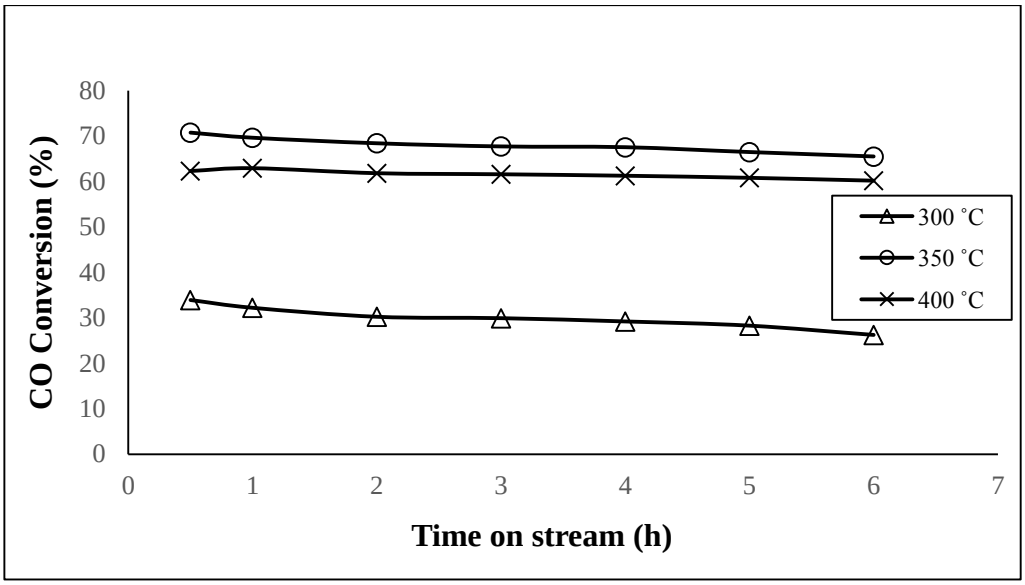

Figure A.3. Temperature dependence of time-on-stream activity data of 1Pt-0.5Re-1V/CeO_2 for real feed #1.

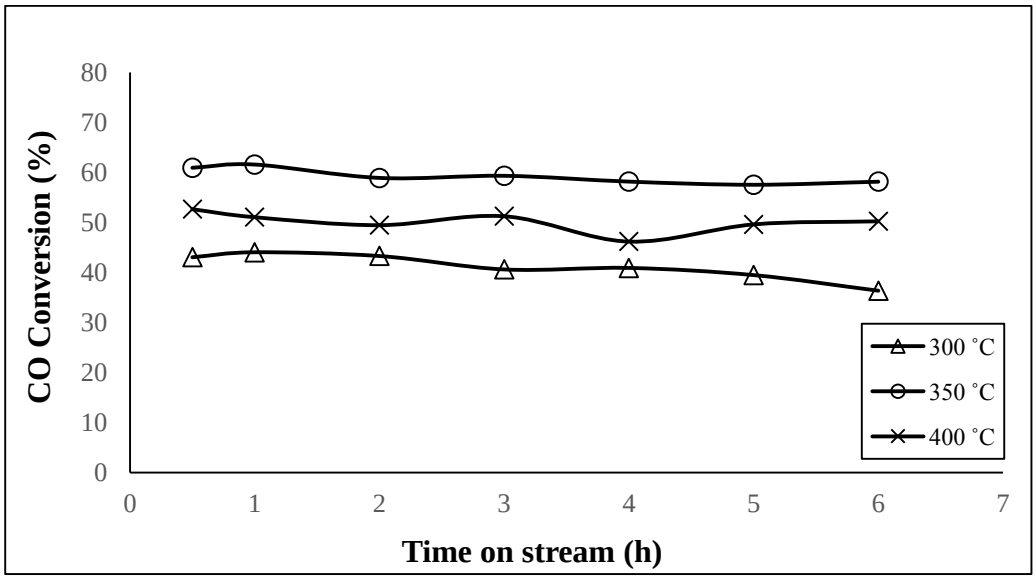

Figure A.4. Temperature dependence of time-on-stream activity data of 0.5Pt-1Re-1V/CeO_2 for real feed #2.

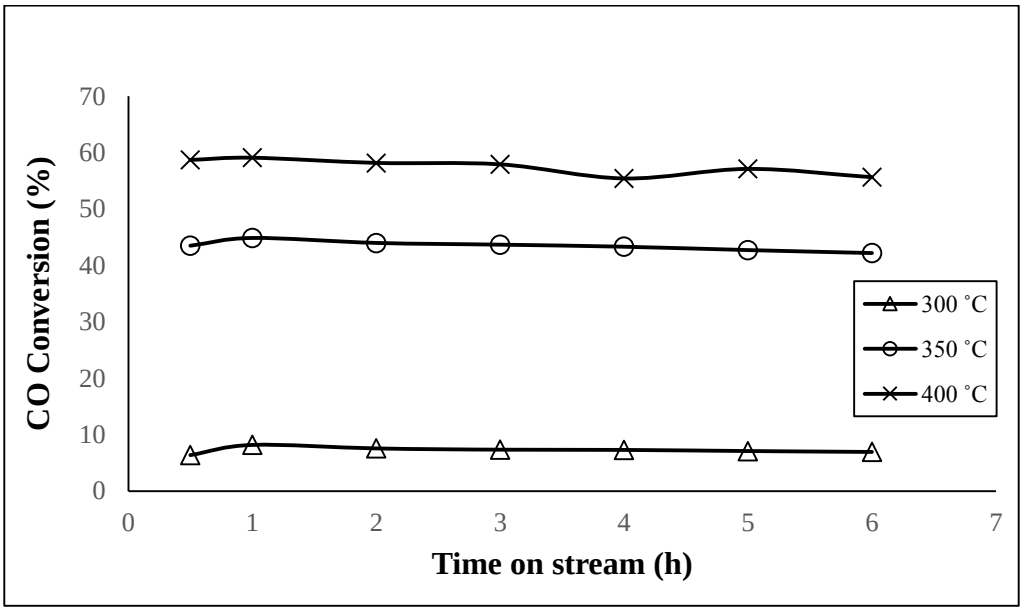

Figure A.5. Temperature dependence of time-on-stream activity data of 0.5Pt-1Re-0.5V/CeO_2 for real feed #1.

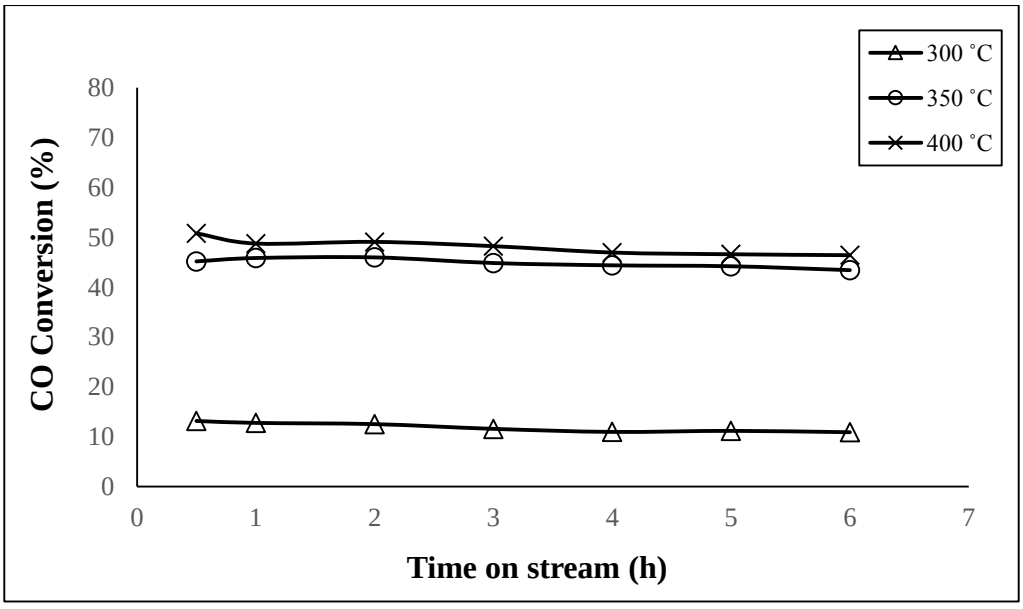

Figure A.6. Temperature dependence of time-on-stream activity data of 0.5Pt-1Re-0.5V/CeO_2 for real feed #2.

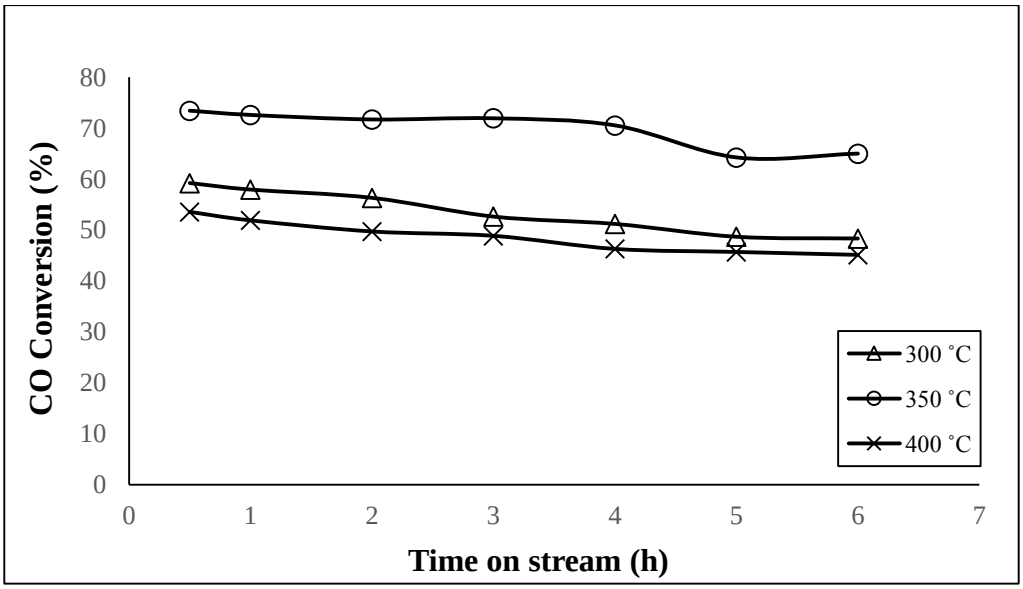

Figure A.7. Temperature dependence of time-on-stream activity data of 1Pt-0.5Re-0.5V/CeO_2 for real feed #1.

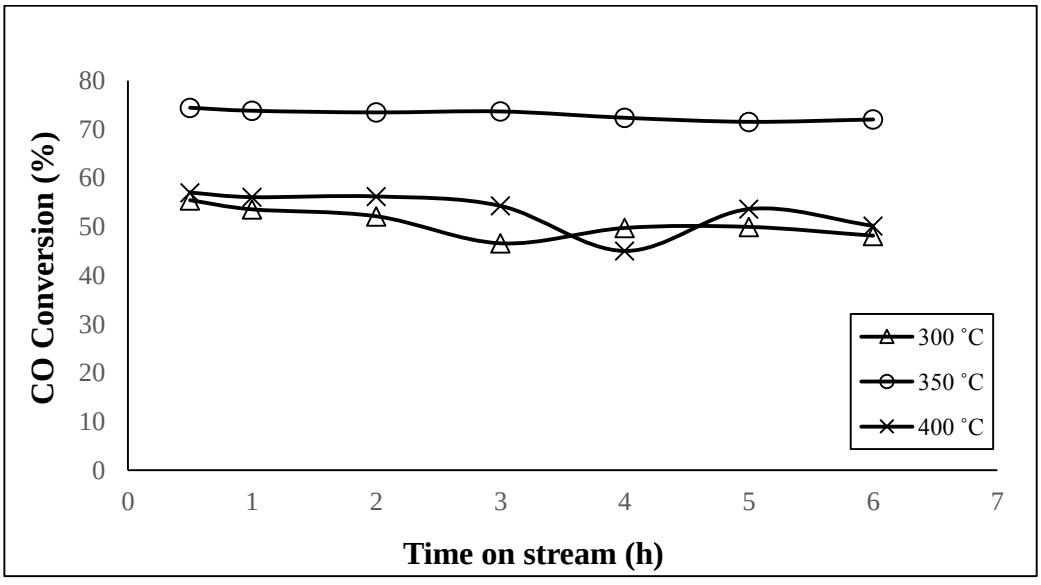

Figure A.8. Temperature dependence of time-on-stream activity data of 1Pt-0.5Re-0.5V/CeO_2 for real feed #2.